doi.org/10.26434/chemrxiv.6097688.v1

A Photoactivatable α5β1-Specific Integrin Ligand

Roshna Vakkeel, Aleeza Farrukh, Aranzazu del Campo

Submitted date: 05/04/2018 • Posted date: 06/04/2018

Citation information: Vakkeel, Roshna; Farrukh, Aleeza; Campo, Aranzazu del (2018): A Photoactivatable α5β1-Specific Integrin Ligand. ChemRxiv. Preprint.

In order to study how dynamic changes of α5β1 integrin engagement affect cellular behaviour, photoactivatable derivatives of α5β1 specific ligands are presented in this article. The presence of the photoremovable protecting group (PRPG) introduced at a relevant position for integrin recognition, temporally inhibits ligand bioactivity. Light exposure at cell-compatible dose efficiently cleaves the PRPG and restores functionality. Selective cell response (attachment, spreading, migration) to the activated ligand on the surface is achieved upon controlled exposure. Spatial and temporal control of the cellular response is demonstrated, including the possibility to in situ activation. Photoactivatable integrin-selective ligands in model microenvironments will allow the study of cellular behavior in response to changes in the activation of individual integrins as consequence of dynamic variations of matrix composition.

File list (1)

A photoactivatable $\alpha_5\beta_1$-specific integrin ligand

Roshna V. Nair,[a] Aleeza Farrukh,[a] Aranzazu del Campo*[a,b]

Abstract: The integrin $\alpha_5\beta_1$ is overexpressed in colon, breast, ovarian, lung and brain tumors and has been identified as key component in mechanosensing. In order to study how dynamic changes of $\alpha_5\beta_1$ engagement affect cellular behaviour, photoactivatable derivatives of $\alpha_5\beta_1$ specific ligands are presented in this article. A photoremovable protecting group (PRPG) was introduced into the ligand structure at a relevant position for integrin recognition. The presence of the chromophore temporally inhibited ligand bioactivity. Light exposure at cell-compatible dose efficiently cleaved the PRPG and restored functionality. The photoactive ligand had an azide end-functional group for covalent immobilization onto biomaterials via click chemistry. Selective cell response (attachment, spreading, migration) to the activated ligand on the surface is achieved upon controlled exposure, at similar levels to the native ligand. Spatial and temporal control of the cellular response is demonstrated, including the possibility to *in situ* activation. Photoactivatable integrin-selective ligands in model microenvironments will allow the study of cellular behavior in response to changes in the activation of individual integrins as consequence of dynamic variations of matrix composition.

Introduction

The interaction between membrane integrins and adhesive and structural proteins on the extracellular matrix (ECM) is fundamental in cellular processes like adhesion or migration.[1] Experimental investigation of these interactions is typically performed using anti-integrin monoclonal Antibodies[2] or peptidomimetica to block or activate individual integrins.[3] Out of 24 different integrin subtypes created by combinations of 18 α and 8 β subunits, almost half of them bind to ECM proteins through the tripeptide Arg-Gly-Asp (RGD), a widely represented adhesive motif in ECM proteins like fibronectin, vitronectin or collagen. Several groups have developed RGD-based ligands with high specificity for individual integrins,[4] Kessler's group being one of the major contributors with peptidomimetics with high affinity and selectivity towards $\alpha_5\beta_1$ and $\alpha_v\beta_3$ integrins,[5] recently expanded to epithelial integrin $\alpha_v\beta_6$.[5b] Although originally developed as antagonists for cancer therapeutics, these ligands have become unique tools to study integrin-mediated adhesion to matrices, and to investigate the individual role of $\alpha_5\beta_1$ and $\alpha_V\beta_3$ in cell adhesion and migration, and their involvement in mechanosensing and mechanotransduction.[6] For example, β_3 integrins have been demonstrated to favour persistent migration and β_1 integrins random migration in fibroblasts.[7] Fibrillar adhesion patterns and increased spreading are observed in cells attached to surface *via* $\alpha_5\beta_1$ ligands, whereas localized focal adhesion clusters at cell margins are obtained in cells adhering to $\alpha_v\beta_3$ ligand.[6a] Activation of $\alpha_5\beta_1$-integrins is associated with high RhoA activity, reduce in actin stress fiber formation and increase in cortical actin assembly.[6a] Cells attached to surface through $\alpha_5\beta_1$ –integrins exert higher forces in comparison to cells spreading due to $\alpha_v\beta_3$ integrins.[6c, 8] Both integrins crosstalk in mechanotransduction processes.[9] $\alpha_5\beta_1$ integrins are responsible for $\alpha_v\beta_3$ recruitment through an inside-out signaling.[6b] $\alpha_5\beta_1$ integrins are necessary for polarization and rigidity sensing of keratocytes after spreading *via* interaction of $\alpha_v\beta_3$ integrins.[10]

All these experiments have been performed in static culture conditions, i.e. by exposing the cells to a predefined concentration of the ligand/s, and without the possibility of dynamic manipulation at later time points during cell culture. Dynamic changes of the ECM composition are, however, associated to physiologically and pathological states in which integrins are known to play relevant roles.[11] In order to mimic these scenarios *in vitro*, advanced strategies that allow on-demand activation or deactivation of the integrin ligand during cell culture are necessary. In the past, we successfully demonstrated a strategy to modulate the activity of the generic integrin binding ligand cyclic[RGDfK] by using light.[12]

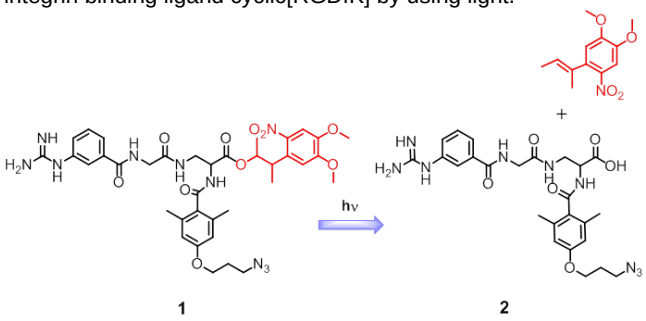

Scheme 1. Structure of phototriggerable $\alpha_5\beta_1$ specific ligand **1** and its photochemical activation reaction with photolysis products.

For this purpose, a photocleavable group was introduced at the carboxylic group of the aspartic acid in the peptide sequence.[12] In this form, the peptide was inactive. Light exposure at cell compatible doses allowed *in situ*, remote and dose-dependent tuning of RGD bioactivity (through the photocleavage of the chromophore), with spatial and temporal control.[13] This was demonstrated in cell cultures and in vivo experiments.[14] However, RGDfK binds to many different integrins and does not allow dynamic integrin-selective studies. In this work, we extend this approach to control the activity of a variant of Kessler's $\alpha_5\beta_1$-specific integrin ligand (**2**, Scheme 1**)**. By attaching a 3-(4,5-Dimethoxy-2-nitrophenyl)-2-butyl ester (DMNPB) photocleavable group to the free carboxylic group, a phototriggerable derivative of **2** was obtained (**1**, Scheme 1). This molecule allows regulation of $\alpha_5\beta_1$ integrin related cellular processes by light exposure. This article describes the synthesis of the key molecule, and the demonstration of light-driven bioactivity in adhesion and migration assays.

[a] R. V. Nair, A. Farrukh, A. del Campo
INM – Leibniz Institute for New Materials, Campus D2 2,
66123 Saarbrücken, Germany
E-mail: Aranzazu.DelCampo@leibniz-inm.de
[b] A. del Campo
Saarland University,
Chemistry Department,
66123 Saarbrücken, Germany

Supporting information for this article is given via a link at the end of the document.

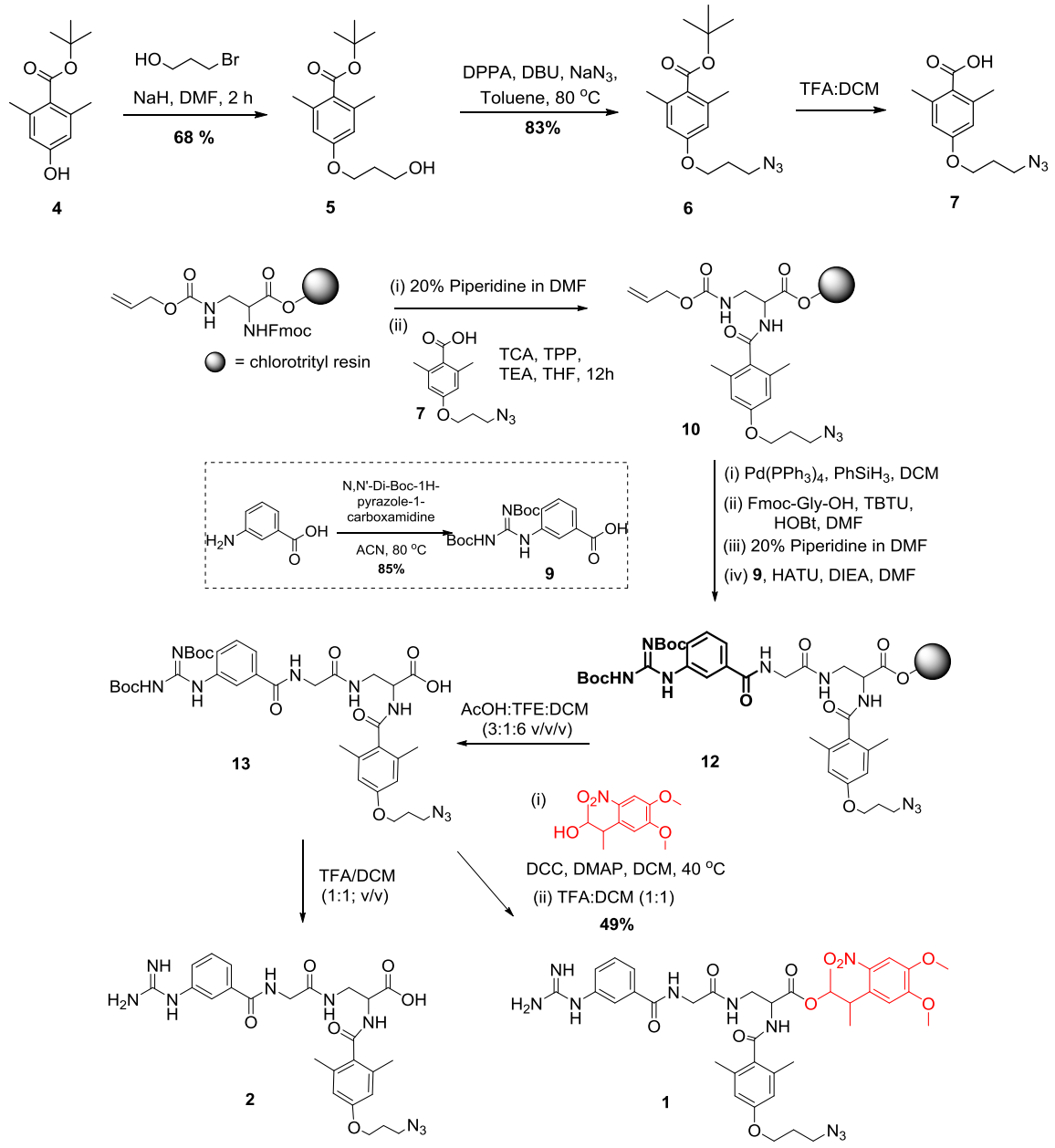

Scheme 2. Synthetic steps involved in preparation of **1** and **2**..

Results and Discussion

Synthesis of photoactivatable $\alpha_5\beta_1$ ligand with surface functionalisable azide group

The synthesis strategy for **1** and **2** was adapted from the method reported by Kessler group.[1] The ligands in this work contain azide groups for later coupling to biomaterials, in contrast to reported ligands from Kessler's group functionalized with thiols.[15] The azide group has reasonable stability against acidic or basic treatments and allows some simplification of protection steps during the synthesis of the molecule **1**.[15] The azide linker was introduced starting from Kessler's intermediate tert-butyl 4-hydroxy-2,6-dimethylbenzoate **4** in only 3 steps (details in Scheme 1 in SI): a simple SN^2 reaction with 1-bromopropanol, followed by azidation of hydroxyl group[16] and deprotection of *tert*-butyl ester. 4-(3-azidopropoxy)-2,6-dimethylbenzoic acid (**7**) was obtained in good yields. Coupling of **7** to Dap(Alloc) on chlorotrityl polystyrene (TCP) resin was performed following the strategy reported by Vágó&Greiner[17] using trichloroacetonitrile and triphenylphosphine in THF. This coupling required long reaction time (12 h), but proceeded to acceptable 60% conversion. The unreacted amines were capped using acetic anhydride. Attempts to couple **7** using agents like HATU, HBTU and PyBrOP were all unsuccessful, even in N-Methyl-2-pyrrolidone (NMP) and DMF as solvents. Attempts to couple 4-(3-(((benzyloxy)carbonyl)amino)propoxy)-2,6-dimethylbenzoic

acid **10a** were also unsuccessful (details in SI, Table S1). For the following coupling steps on the resin, DMF was used as solvent and Kessler's conditions were used.[5b] Another deviation from Kessler`s method was the coupling of diBoc-protected guanidylated 3-aminobenzoic acid (**9**) to **11** to obtain **12** in good yield. Synthesis of **9** from 3-amino benzoic acid in chloroform failed, but synthesis in dry acetonitrile was successful. The protected guanidine group was necessary in order to avoid interference with the coupling of the DMNPB group at later step. The cleavage of the molecule from the resin to obtain **13** with intact diBoc-protected guanidine group was a crucial step. The use of chlorotrityl resin (TCP) was necessary, as TCP allows cleavage the molecule from the resin under mild conditions. Reaction of **13** with 3-(4,5-Dimethoxy-2-nitrophenyl)-2-butyl ester (DMNPB) and subsequent deprotection of Boc groups of guanidine afforded the targeted molecule **1**. The active ligand **2** was easily obtained from **13** after deprotection step. The final products were isolated with high purity and characterized. Details on the synthetic protocols and characterization are provided in the supporting information, together with information about alternative routes taken for the synthesis of the intermediates.

Photochemical properties of photoactivatable $\alpha_5\beta_1$ ligand (1)

The photolysis of **1** in solution was followed by UV spectrophotometry and HPLC. A 0.5 mM solution of **1** in water was irradiated at λ_{max} = 360 nm (2.7 mW/cm^2) at increasing exposure times. The UV spectra showed a slight increase and broadening of the absorption maximum (λ_{max} = 346 nm) (Figure S1) was observed. This change is associated to the decreasing concentration of DMNPB and the increasing concentration of photolytic byproduct. Aliquots of 20 µL were taken at different time intervals and the composition of the irradiated mixture was analyzed by quantitative HPLC. The HPLC peak corresponding to **1** (t_r = 27.1 min) decreased in intensity with increasing exposure time, while a new peak with increasing intensity appeared at t_R = 19.2 min. This peak showed absorption only in 210 nm and 254 nm channels, but not in 360 nm, indicating that DMNPB chromophore was not part of its structure (**Figure 1a**). Mass analysis confirmed that the new peak corresponded to the activated ligand **2**. In order to quantify the concentration of **2** liberated in the solution, a calibration curve was established and the area% of the peaks with tr = 19.2 min was interpolated. A conversion degree of 92% was measured at full exposure (**Figure 1b**). This high chemical yield and the clean photolysis reaction are relevant properties for a successful application of **1** in the following biological experiments.

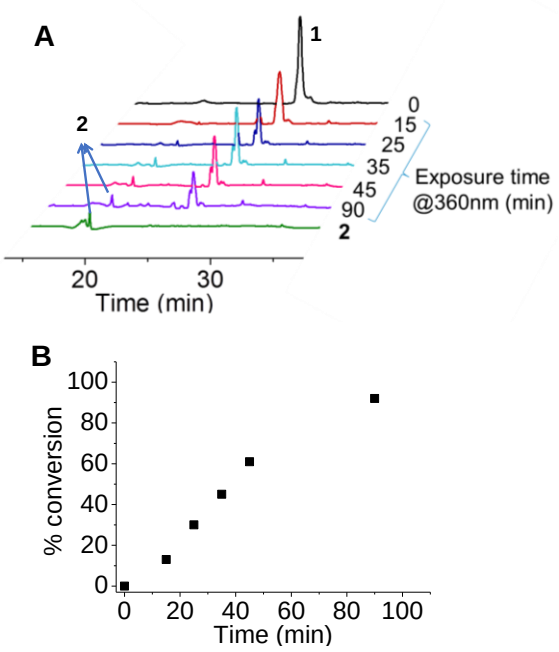

Figure 1. A HPLC profiles of a 0.5 mM solution of **1** in water at different exposure time at 360 nm (2.7 mW/cm^2). Elugrams were recorded with 210 nm channel in HPLC. **B** Conversion degree of the photolysis of **1**.

Bioactivity of photoactivatable $\alpha_5\beta_1$ ligand

In order to test the bioactivity of the synthesized ligands **1** and **2**, these were used to derivatize commercially available Nexterion® H slides for studies of cell responses. Nexterion H slides have NHS-activated carboxy-terminated PEGylated surfaces, which were converted into dibenzocyclooctyne (DBCO) groups by reaction with Dibenzocyclooctyne-amine in DMSO. Incubation of the substrates with compounds **1** or **2** is expected to click the ligands to the surface *via* copper-free azide-alkyne cycloaddition reaction.

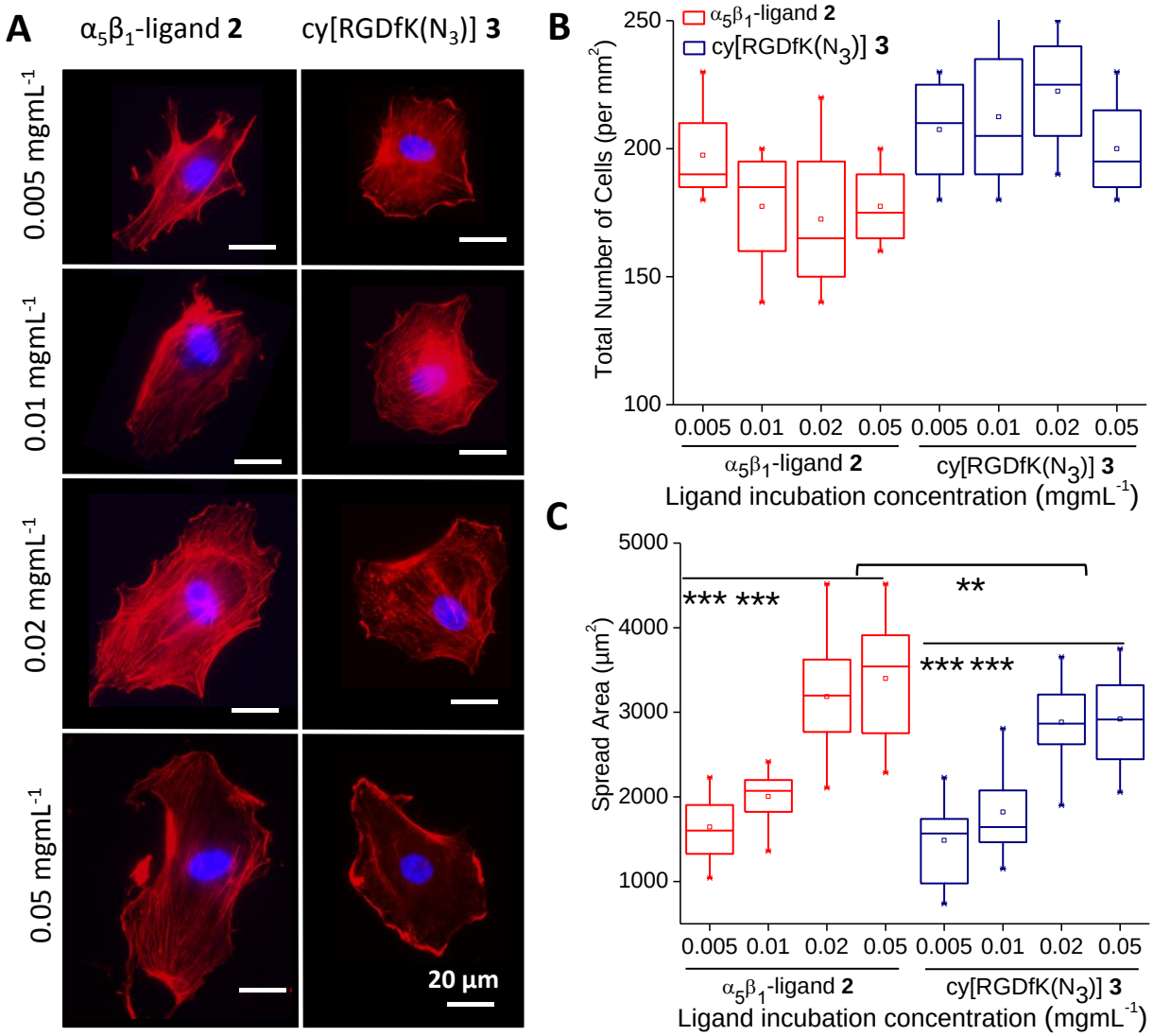

Figure 2. A. Immunofluorescence images of HUVECs after 24 h of culture on $\alpha_5\beta_1$-ligand **2** and cyclo[RGDfK(N_3)] **3** modified substrate at increasing ligand densities. Actin fibers were stained with Phalloidin TRITC and nucleus with DAPI. **B.** Quantification of the cell density on the surface. **C**. Quantification of cell spreading. Statistical significance was analyzed by Tukey- test shows significant differences between different concentrations and different ligands. Significance was calculated by comparison of difference concentrations to 0.05 mgmL^{-1}, and between the ligand in comparison with $\alpha_5\beta_1$-ligand (mean ± SD, ANOVA, ** p <0.01, *** p <0.001). No statistically significant difference was observed in total number of cells in all tested conditions.

Initially different incubation concentrations of $\alpha_5\beta_1$-ligand 2 (0.005 – 0.05 mgmL^{-1}) were used in order to determine the optimal concentration to which cells respond. HUVECs were cultured on functionalized substrates for 24h, fixed and imaged. Cell attachment was observed on all substrates. The number of adhered cells per given area was not significantly different at the different ligand concentrations tested, and even showed a slight decrease at higher concentrations (Figure 2B). This decrease was associated with significant increase of spreading area observed for incubation concentrations above 0.02 mgmL^{-1} (Figure 2C). These results demonstrate that the exchange of the thiol linker by azide in Kessler's $\alpha_5\beta_1$ specific adhesive ligand[15] does not affect its activity.

Substrates modified with $\alpha_5\beta_1$-ligand **2** (0.02 mgmL^{-1} incubation concentration) were then taken for further studies, and cell behavior over time was observed by live cell imaging (**Figure 3A**). Within the first 15 minutes more than 60% of cells already attached on the substrate (**Figure 3C**), and significant spreading was visible within one hour (**Figure 3D**), indicating very fast cellular response to the ligand. Fast spreading kinetics was also reported for the thiol-derivatized ligand in Kessler's work.[5c, 15, 18] The morphology of HUVECs quickly changed within the first 3h from circular to more elongated shape, and remained unchanged during rest of cell culture (**Figure 3A**).

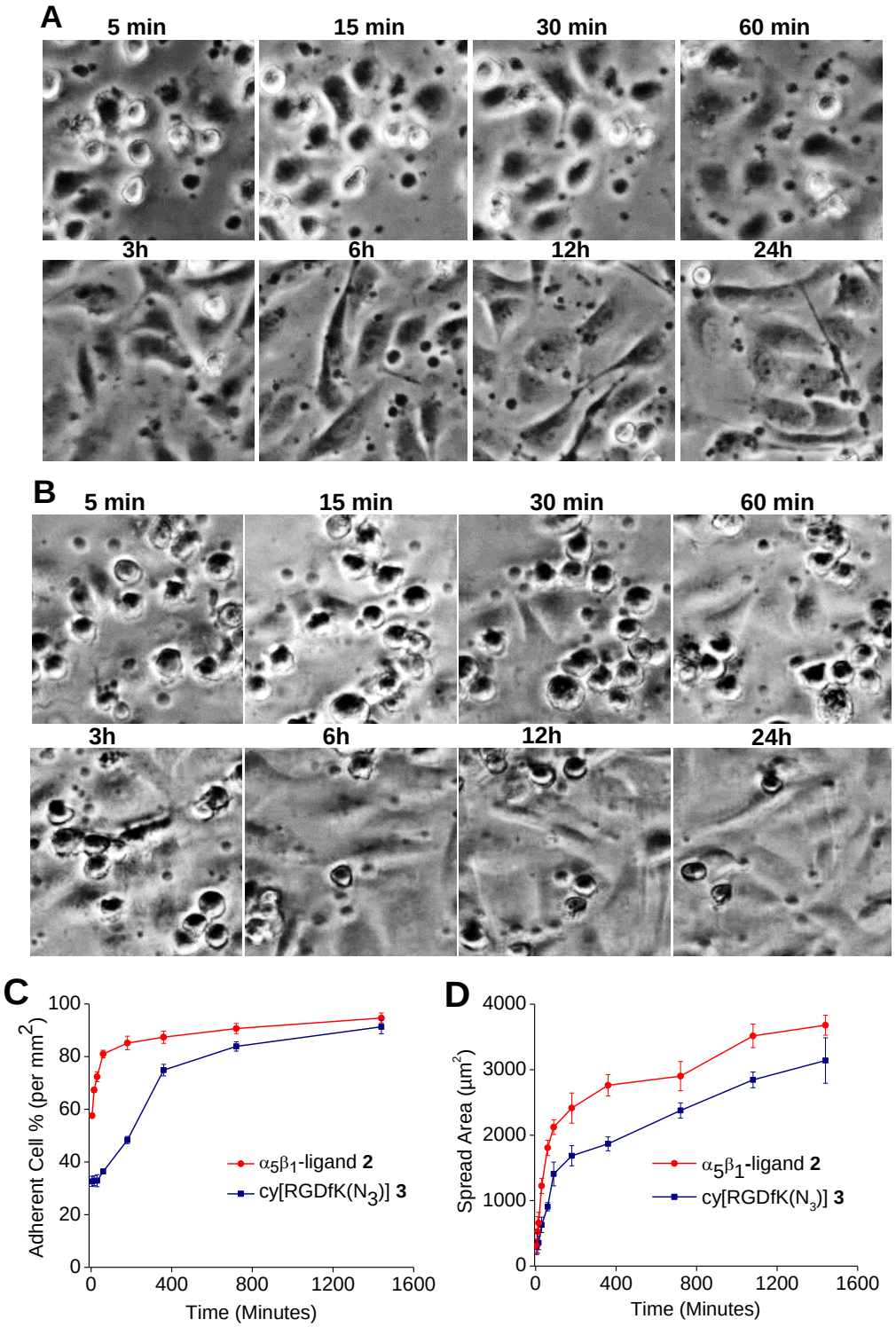

Figure 3. A, B: Phase contrast microscopy images of time lapse experiment over 24 hours showing the morphology of HUVECs cultured on Nexterion H slides functionalized with $\alpha_5\beta_1$-ligand **2** (A) or cy[RGDfK(N_3)] **3** (B) ligands (incubation concentration 0.02 mgmL^{-1}). **C, D:** Quantification of adherent cells and cell spreading area at different time points..

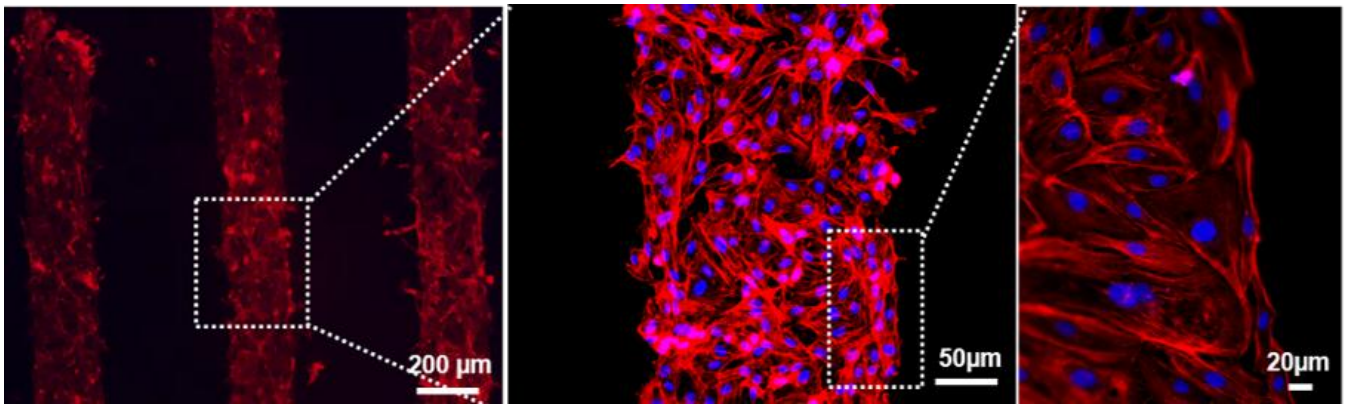

Figure 4. Site-selective adhesion of HUVECs on substrates functionalized with ligand **1** irradiated through quartz mask with 600 µm chrome stripe patterns separated by 300 µm gaps. HUVECs attach selectively to the exposed areas, where the ligand was activated. Images were taken 24 hours after seeding. Actin was stained with Phalloidin TRITC (red) and nucleus was stained with DAPI (blue).

For comparison, similar experiments were performed with the widely used RGD eptidemotif using the azide-derivatized cyclo[RGDfK(N_3)] (**3,** structure in SI). This ligand binds to different integrins, including $\alpha_5\beta_1$. Cell attachment kinetics was significantly faster on $\alpha_5\beta_1$-ligand than on cy[RGDfK(N_3)]. A 40% higher number of adherent cells was measured on $\alpha_5\beta_1$-ligand after one hour of cell culture, though the difference vanished at longer culture times (Figure 3C). HUVECS show ~1 fold faster spreading on $\alpha_5\beta_1$-ligand than on cy[RGDfK(N_3)] during 1h of culture. This trend prevailed over 24h, when a 20% higher cell spreading was measured on $\alpha_5\beta_1$-ligand modified substrates (Figure 3D). Cells showed polarized and elongated morphology on $\alpha_5\beta_1$-ligand **2**, with more longitudinally oriented actin network in comparison to relatively randomly distributed actin fibers on cy[RGDfK(N_3)] (Figure 2A). These differences in the interaction of cells with $\alpha_5\beta_1$-specific ligand *vs* unspecific RGD motif reflect the different roles of integrins in adhesion.[18-19] These results foresee the possibility to manipulate cellular processes by regulating integrin-related signals using photoactivatable integrin-selective ligands.

The possibility to regulate the bioactivity of $\alpha_5\beta_1$-ligand **2** with the photoactivatable-$\alpha_5\beta_1$ variant **1** was then evaluated. HUVECs were seeded on substrates modified with photoactivatable-$\alpha_5\beta_1$ variant **1** (incubation concentration 0.02 mgmL^{-1}). No cell attachment was observed, indicating successful blocking of the binding site with the DMNPB chromophore and inhibition of integrin binding and integrin-mediated cell adhesion. On photoactivated samples, cells attached and spread in similar manner to positive controls (Figure S2). When substrates were irradiated trough a mask, cells selectively adhered to the exposed areas, with active $\alpha_5\beta_1$-ligand present now on the surface, forming well-defined patterns (Figure 4). The spatial selectivity was retained during 4 days of culture, demonstrating that **1** is stable against hydrolysis in cell culture conditions, and is photostable enough to allow culture under normal incubation conditions and during imaging. Cells on irradiated samples of functionalized with **1**, showed similar adhesion and spreading levels and kinetics to native $\alpha_5\beta_1$-ligand. All together, these results demonstrate that the introduction of the DMNPB photocleavable group at the carboxylic group of $\alpha_5\beta_1$ ligand temporary blocks the bioactivity of the ligand. The activity can be fully restored after light exposure.

Finally, the possibility to *in situ* activation of **1** in the presence of cells using a scanning laser was tested. Patterned monolayers of HUVECs (as in Figure 4) were placed in the cell chamber of a microscope, Using a scanning laser at 405 nm, lines of 40 µm width and 250 µm length were irradiated between the endothelial patterned monolayers. Note that these areas were not exposed in previous masked irradiation step and, therefore photoactivatable-$\alpha_5\beta_1$-ligand **1** was present in a latent form. Already 5 minutes after activation, migration of individual cells was observed along the scanned lines, confirming the *in situ* activation of the $\alpha_5\beta_1$ ligand. Cells detached from the monolayer and migrated along de line until they reached the other edge, approximately in 5h (Figure 5). Cell showed persistent migration with speed of ca. 3 µm/min speed (Figure S3).

Conclusions

In conclusion, a phototriggerable variant of $\alpha_5\beta_1$ antagonist with an azide terminated linker was successfully synthesized. The covalently attached DMNPB chromophore at the COOH group allowed inhibition of the biological activity of the ligand, and efficient photolysis and reactivation at cell compatible light doses. Masked-irradiated substrates modified with **1** allowed site-selective attachment of HUVECs to the photoactivated areas. Cell adhesion and spreading levels and kinetics were similar to those of native $\alpha_5\beta_1$ ligand, in agreement with the high photochemical yield observed on the HPLC studies of irradiated solutions. These results evidence the potential of photoactivatable-$\alpha_5\beta_1$-ligand **1** as tool to study $\alpha_5\beta_1$-dependent processes in cell biology by allowing precise control of its presence and concentration in time and space.

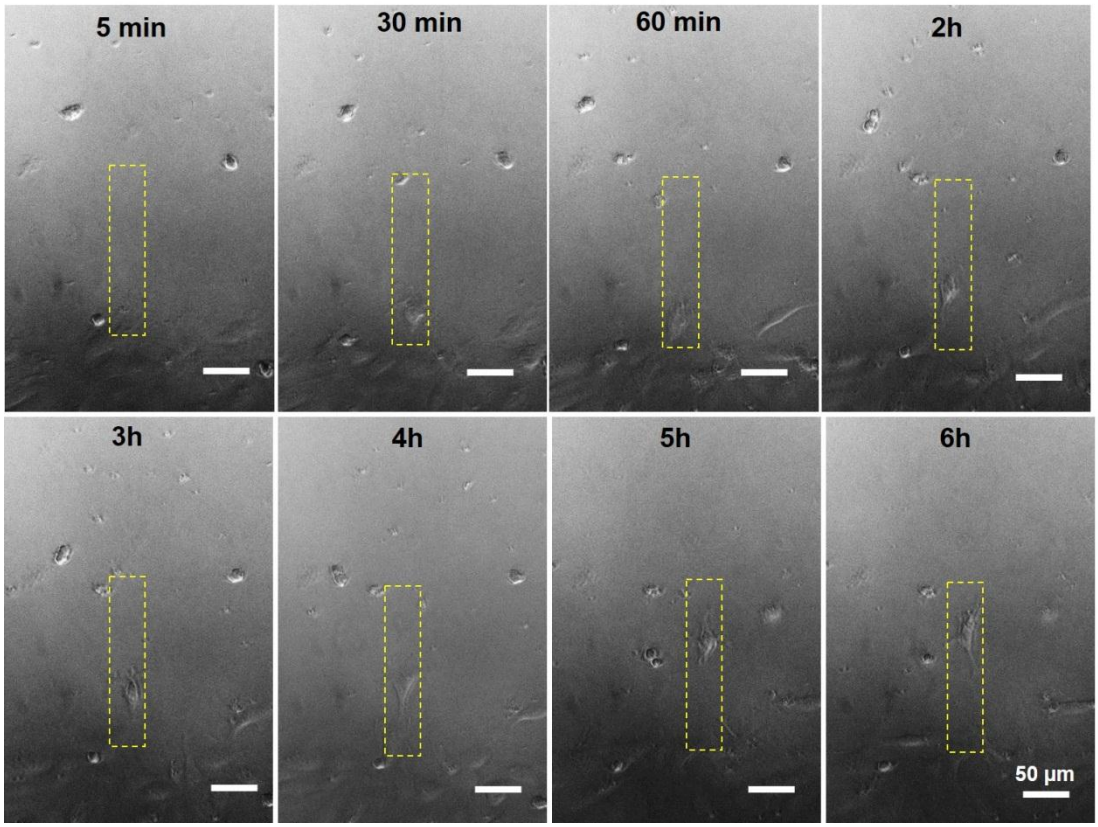

Figure 5. Light-triggered migration of HUVECs from the monolayer into $\alpha_5\beta_1$ activated lines using a scanning laser.

Experimental Section

Cell culture

Human umbilical vein endothelial cells (HUVECs) (Promocell) were cultured in M199 basal medium (Sigma, M4530) and supplemented with L-glutamine (2 mM), penicillin (1000 U/L), streptomycin (100 mg/L, Sigma), ECGS supplement (Sigma, E-2759), sodium heparin (Sigma, H-3393) and 20% fetal calf serum (FCS) as previously described.[3] HUVEC were used between passages 2 to 6.

Nexterion® H glass slide functionalized with different concentration of ligand (photoactivatable-$\alpha_5\beta_1$-ligand 1, $\alpha_5\beta_1$-ligand 2 and cy[RGDfK(N_3)]) divided by 12-well silicon gasket, were seeded with 3×10^4 cells/well suspension of HUVECs at 37 °C and 5% CO_2. Cells were cultured for 24h and fixed with 4% PFA solution, permeabilized with 0.5% Triton, actin fibers were stained with TRITC-phalloidin (1:200) and DAPI (1:500) to stain nucleus the samples were mounted with mounting medium (Dinova) by using standard protocols. Fluorescence images were taken with Zeiss Axio Observer epi-fluorescence microscope.

Alternatively, samples were monitored by time-lapse microscopy for 24h by taking pictures every 5 min on Zeiss Axio observer microscope, equipped with CO_2 and heating unit.

For cell experiments of photoactivatable-$\alpha_5\beta_1$-ligand 1 functionalized samples without light activation, full pre-irradiation or irradiation through mask, 4×10^4 HUVECs were seeded/well. The medium was changed after 12 h to remove the unattached cells and cells were kept in culture till four days. Samples were fixed with with 4% PFA solution and stained with TRITC-phalloidin and DAPI by using standard protocol as described above. Fluorescence images were taken with Zeiss Axio Observer epi-fluorescence microscope.

Statistical Analysis

Data were expressed as mean ± standard deviation. For each condition, a minimum of three independent experiments were performed with sample size larger than 10 fields in all cases. The value of $p < 0.05$ was used for statistical significance. A one-way ANOVA with a Tukey test of the variance was used to determine the statistical significance between groups. The statistical significance difference was set to* $\alpha< 0.05$, **$\alpha< 0.01$, ***$\alpha< 0.001$.

Acknowledgements

Authors thank Dr. Dimitri Missirlis (Heidelberg University) for fruitful discussions on the ligand activity.

Keywords: $\alpha_5\beta_1$ integrin • peptidomimetics • cell adhesive ligand • phototriggers.

References

[1] U. K. Marelli, F. Rechenmacher, T. R. Sobahi, C. Mas-Moruno, H. Kessler, *Front Oncol* **2013**, *3*, 222.

[2] A. Byron, J. D. Humphries, J. A. Askari, S. E. Craig, A. P. Mould, M. J. Humphries, *J. Cell Sci.* **2009**, *122*, 4009.

[3] A. Tolomelli, P. Galletti, M. Baiula, D. Giacomini, *Cancers* **2017**, *9*, 78.

[4] aK. Ley, J. Rivera-Nieves, W. J. Sandborn, S. Shattil, *Nat Rev Drug Discov* **2016**, *15*; bM. Pilkington-Miksa, E. M. V. Araldi, D. Arosio, L. Belvisi, M. Civera, L. Manzoni, *Org. Biomol. Chem.* **2016**, *14*, 3221-3233.

[5] aT. G. Kapp, F. Rechenmacher, S. Neubauer, O. V. Maltsev, E. A. Cavalcanti-Adam, R. Zarka, U. Reuning, J. Notni, H.-J. Wester, C. Mas-Moruno, J. Spatz, B. Geiger, H. Kessler, *Sci. Rep.* **2017**, *7*, 39805; bD. Heckmann, A. Meyer, B. Laufer, G. Zahn, R. Stragies, H. Kessler, *Chembiochem* **2008**, *9*, 1397-1407; cC. Mas-Moruno, R. Fraioli, F. Rechenmacher, S. Neubauer, T. G. Kapp, H. Kessler, *Angew. Chem. Int. Ed.* **2016**, *55*, 7048-7067.

[6] aV. Schaufler, H. Czichos-Medda, V. Hirschfeld-Warnecken, S. Neubauer, F. Rechenmacher, R. Medda, H. Kessler, B. Geiger, J. P. Spatz, E. A. Cavalcanti-Adam, *Cell Adh. Migr.* **2016**, *10*, 505-515; bJ. Guasch, B. Conings, S. Neubauer, F. Rechenmacher, K. Ende, G. Rolli Claudio, C. Kappel, V. Schaufler, A. Micoulet, H. Kessler, H. G. Boyen, A. Cavalcanti‐Adam Elisabetta, P. Spatz Joachim, *Adv. Mater.* **2015**, *27*, 3737-3747; cS. Rahmouni, A. Lindner, F. Rechenmacher, S. Neubauer, A. Sobahi Tariq Rashad, H. Kessler, A. Cavalcanti‐Adam Elisabetta, P. Spatz Joachim, *Adv. Mater.* **2013**, *25*, 5869-5874.

[7] D. Missirlis, T. Haraszti, C. v. C. Scheele, T. Wiegand, C. Diaz, S. Neubauer, F. Rechenmacher, H. Kessler, J. P. Spatz, *Sci. Rep.* **2016**, *6*, 23258.

[8] L. Lin Grace, M. Cohen Daniel, A. Desai Ravi, T. Breckenridge Mark, L. Gao, J. Humphries Martin, S. Chen Christopher, *FEBS Lett.* **2013**, *587*, 763-769.9] Z. Sun, S. S. Guo, R. Fässler, *J. Cell Biol.* **2016**.[10] aM. Riaz, M. Versaevel, D. Mohammed, K. Glinel, S. Gabriele, *Sci. Rep.* **2016**, *6*, 34141; bP. Roca-Cusachs, N. C. Gauthier, A. Del Rio, M. P. Sheetz, *Proc Natl Acad Sci U S A* **2009**, *106*, 16245-16250; cN. Strohmeyer, M. Bharadwaj, M. Costell, R. Fässler, D. J. Müller, *Nat. Mater.* **2017**, *16*, 1262.

[11] A. Starchenko, R. Graves-Deal, Y.-P. Yang, C. Li, R. Zent, B. Singh, R. J. Coffey, *Mol. Biol. Cell* **2017**, *28*, 1288-1300.

[12] S. Petersen, J. M. Alonso, A. Specht, P. Duodu, M. Goeldner, A. del Campo, *Angew. Chem., Int. Ed.* **2008**, *47*, 3192-3195.

[13] aA. Specht, F. Bolze, Z. Omran, J. F. Nicoud, M. Goeldner, *HFSP J* **2009**, *3*, 255-264; bM. J. Salierno, A. J. García, A. del Campo, *Adv. Funct. Mater.* **2013**, *23*, 5974-5980.

[14] T. T. Lee, J. R. García, J. I. Paez, A. Singh, E. A. Phelps, S. Weis, Z. Shafiq, A. Shekaran, A. del Campo, A. J. García, *Nat. Mater.* **2014**, *14*, 352.

[15] F. Rechenmacher, S. Neubauer, J. Polleux, C. Mas-Moruno, M. De Simone, E. A. Cavalcanti-Adam, J. P. Spatz, R. Fassler, H. Kessler, *Angew. Chem. Int. Ed.* **2013**, *52*, 1572-1575.

[16] A. S. Thompson, G. R. Humphrey, A. M. DeMarco, D. J. Mathre, E. J. J. Grabowski, *J. Org. Chem.* **1993**, *58*, 5886-5888.

[17] I. Vágó, I. Greiner, *Tet. Lett.* **2002**, *43*, 6039-6041.

[18] D. Missirlis, T. Haraszti, C. v. C. Scheele, T. Wiegand, C. Diaz, S. Neubauer, F. Rechenmacher, H. Kessler, J. P. Spatz, *Scientific reports* **2016**, *6*, 23258.

[19] V. Schaufler, H. Czichos-Medda, V. Hirschfeld-Warnecken, S. Neubauer, F. Rechenmacher, R. Medda, H. Kessler, B. Geiger, J. P. Spatz, E. A. Cavalcanti-Adam, *Cell adhesion & migration* **2016**, *10*, 505-515.

Supporting Information

A photoactivatable $\alpha_5\beta_1$-specific integrin ligand

Roshna V. Nair,[a] Aleeza Farrukh,[a] Aranzazu del Campo*[a,b]

[a] INM – Leibniz Institute for New Materials, Campus D2 2, 66123 Saarbrücken, Germany
[b] Saarland University, Chemistry Department, 66123 Saarbrücken, Germany

(*)Corresponding author:
Prof Dr A. del Campo: Tel: +49(0)681-9300-510, Fax +49(0)681-9300-223,
E-mail: aranzazu.delcampo@leibniz-inm.de. ORCID: 0000-0001-5725-2135

Keywords: $\alpha_5\beta_1$ integrin, peptidomimetics, cell adhesive ligand, phototriggers.

General Procedures and Synthesis

Solvents and Reagents.

Chemicals and solvents were purchased from Fluka Chemie AG (D-82024 Taufkirchen), Merck KGaA (D-64271 Darmstadt), ABCR (D-76189 Karlsruhe), Acros Organics (B-2440 Geel) and Sigma-Aldrich Chemie GmbH (D-89555 Steinheim). Solvents had p.a. purity and were used as purchased unless specified. Protected Fmoc protected amino acids, coupling reagents and solid phase peptide synthesis resin were purchased from Novabiochem (Schwalbach, Germany), Iris Biotech GmbH (Marktredwitz, Germany).

Characterisation methods

Analytical thin layer chromatography was performed with TLC plates (ALUGRAM® SIL G/ UV254) from Macherey-Nagel, Germany. Column chromatography was carried out using Merck silica gel (60Å pore size, 63-200 μm particle size).

[a] R. V. Nair, A. Farrukh, A. del Campo
INM – Leibniz Institute for New Materials, Campus D2 2,
66123 Saarbrücken, Germany
E-mail: Aranzazu.DelCampo@leibniz-inm.de
[b] A. del Campo
Saarland University,
Chemistry Department,
66123 Saarbrücken, Germany

The components were visualized using an UV lamp (254nm). A JASCO HPLC PU-4086 series equipped with a diode array UV-Vis detection system, fraction collector and a semi-preparative column (100 mm C18) filled with Reprosil RP18 (5 μm grain size, 250 x 20 mm) was used for purification of final compounds. For analytical HPLC a column (250 mm x 4.6 mm) filled with the same material was used. Solution ^{1}H- and ^{13}C-NMR spectra were recorded on a Bruker Avance 300 (300MHz). Chemical shifts (δ) are given in parts per million (ppm). NMR spectra measurements were made at room temperature with reference of TMS (δ= 0 ppm). The chemical shifts are provided in parts per million and the coupling constants in Hertz. The following abbreviations are used: *s*-singlet, *t*-triplet, *q*-quartet, *m*-multiplet. Mass spectra were recorded with Agilent Technologies InfinityLab Liquid Chromatography/Mass Selective Detector (LC/MSD) and 6500 Series Accurate-Mass Quadrupole Time-of-Flight (Q-TOF) LC/MS using electrospray chemical ionisation. Varian Cary 4000 UV/VIS spectrometer (Varian Inc. Palo Alto, USA) was used to record UV/VIS Spectra in Quartz cuvettes that were sonicated in THF and Milli-Q water and dried in a N_2 stream before measurement.

Synthesis

General Procedures (GP)

GP1 - Fmoc deprotection

Fmoc protected peptide bound to the resin was treated with 20% piperidine in DMF (v/v) for 5 min. After draining the solution, the same soltion was drawn into the syringe and was shaken for next 15 min. The resin was washed with DMF (5x).

GP2 – Coupling of protected amino acid and resin-bound free amine with HATU/TBTU/HBTU

The solution of the protected amino acid (2 eq.), HATU/TBTU/HBTU (2 eq.), HOBt (2 eq.), DIEA (5 eq.) in DMF was added to the resin-bound free amine and shaken for 2 h at room temperature. The resin was later washed with DMF (5x) after the coupling mixture was drained.

GP3 - Cleavage from 2-Chlorotrityl chloride resin (100-200 mesh), 1% DVB resin

The resin-bound compound was treated with acetic acid, 2,2,2-triflouroethanol and DCM (3:1:6 v/v/v) for 20 min (3x). The collected solutions were pooled together and concentrated *in vacuo*.

GP4 – Deprotection of Boc or *tert*-butyl ester groups

Boc protected compound or tert-butyl analogue (0.1 g) is treated with TFA/DCM (3 mL:3 mL, 1:1; v/v) and stirred for 30 min. The solvent was removed under reduced pressure to obtain the deprotected amine (Boc removal) or carboxylic acid (t-butyl ester) groups.

tert-butyl 4-hydroxy-2,6-dimethylbenzoate (4): Preparation of compound **4** was according to literature starting from 1-((4-bromo-3,5-dimethylphenoxy)methyl)benzene.[1]

tert-butyl 4-(3-hydroxypropoxy)-2,6-dimethylbenzoate (5): To a solution of sodium hydride (0.89 g NaH 60% in paraffin suspension, 2.7 mmol, 1.2 equiv.) in DMF maintained at 0°C, 0.5 g of **4** (2.25 mmol, 1 equiv.) was added portionwise. After 30 minutes stirring at 0 °C, 1-bromopropanol (0.24 ml, 1.2 equiv.) was added dropwise. Reaction was allowed to proceed for 30 min at 0°C, then the cooling bath was removed and the reaction mixture was stirred 2 hour at r.t. After completion of reaction monitored by TLC, 100 ml of saturated solution of NH_4Cl was added, the aqueous layer was extracted twice with 100 ml ethyl acetate, then the combined organic layers were washed with brine and dried over $MgSO_4$. The solvent was removed in vacuum and compound was purified using column chromatography (25% ethyl acetate in hexane) to afford the product **5** as colorless oil (0.43 g, yield 68%). TLC R_F (Hexane/EtOAc: 50/50) = 0.4. ^{1}H-NMR (300 MHz, $CDCl_3$): δ/ppm = 6.55 (1H, s); 4.11-4.07 (2H, t, J= 6 Hz); 3.86-3.82 (2H, t, J= 6 Hz); 2.32 (6H, s); 2.06-1.98 (m, 2H); 1.58 (s, 1H). ^{13}C-NMR (75 MHz, $CDCl_3$): δ/ppm = 169.16, 158.77, 136.76, 128.29, 113.56, 81.39, 65.66, 60.50, 31.93, 28.27, 20.05.

tert-butyl 4-(3-azidopropoxy)-2,6-dimethylbenzoate (6): Procedure for azidation was followed from the procedure reported by Thompson *et al*.[2] To a solution of **5** (0.4 g, 1.4 mmol, 1 equiv.) in DMF maintained at 0 °C, 1,8-Diazabicyclo(5.4.0)undec-7-ene (0.3 ml, 2.1 mmol, 1.5 equiv.) was added followed diphenylphosphoryl azide (0.4 g, 2.1 mmol, 1.5 equiv.). To the reaction mixture, sodium azide (0.27 g, 4.2 mmol, 3 equiv.) was added. After stirring at room temperature for 15 minutes, reaction is then heated at 80 °C for 12 h. The mixture is quenched by water (2 x 10 mL) followed by 5% HCl (10 mL). The compound is then extracted into DCM (2 x 50 mL), and then the combined organic layer is washed with brine. The solvent was removed in vacuum and compound was purified using column chromatography (20% ethyl acetate in hexane) to afford the product **6** as colorless oil (0.36 g, yield 83%). TLC R_F (Hexane/EtOAc: 60/40) = 0.5. ^{1}H-NMR (300 MHz, $CDCl_3$): δ/ppm = 6.54 (1H, s); 4.04-4.00 (2H, t, J= 6 Hz); 3.52-3.47 (2H, t, J= 6 Hz); 2.32 (6H, s); 2.06-1.98 (m, 2H); 1.58 (s, 1H). ^{13}C-NMR (75 MHz, $CDCl_3$): δ/ppm = 169.13, 158.66, 136.77, 128.34, 113.54, 81.40, 64.35, 48.22, 28.76, 28.27, 20.05.

4-(3-azidopropoxy)-2,6-dimethylbenzoic acid (7): The prepared tert-butyl analogue is subjected to deprotection using strategy as described in **GP4** to obtain acid analogue **7**. ^{1}H-NMR (300 MHz, $CDCl_3$): δ/ppm = 6.60 (1H, s); 4.07-4.04 (2H, t, J= 6 Hz); 3.54-3.49 (2H, t, J= 6 Hz); 2.44 (6H, s); 2.09-2.00 (m, 2H); 1.58 (s, 1H). ^{13}C-NMR (75 MHz, $CDCl_3$): δ/ppm = 173.42, 159.62, 139.17, 124.42, 114.07, 64.38, 48.17, 28.72, 28.27, 21.11.

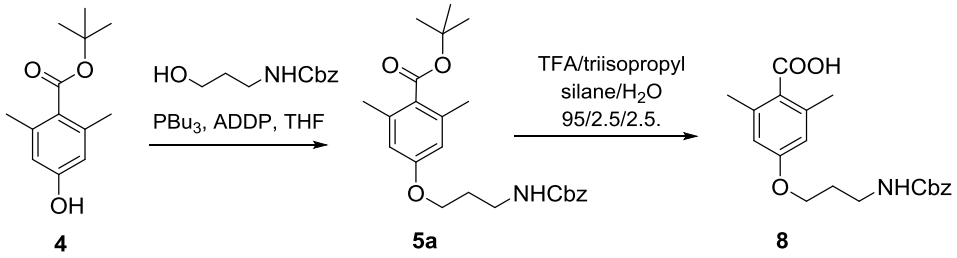

Scheme S1: Synthetic route for aromatic subunit **8**. Synthesis of **8** was achieved starting from compound **4** following Mitsunobu reaction to obtain **5a** followed by **GP4**. (Rechenmacher et al., 2013).

Table S1: Coupling conditions attempted for solid phase synthesis of **10 and 10a.**

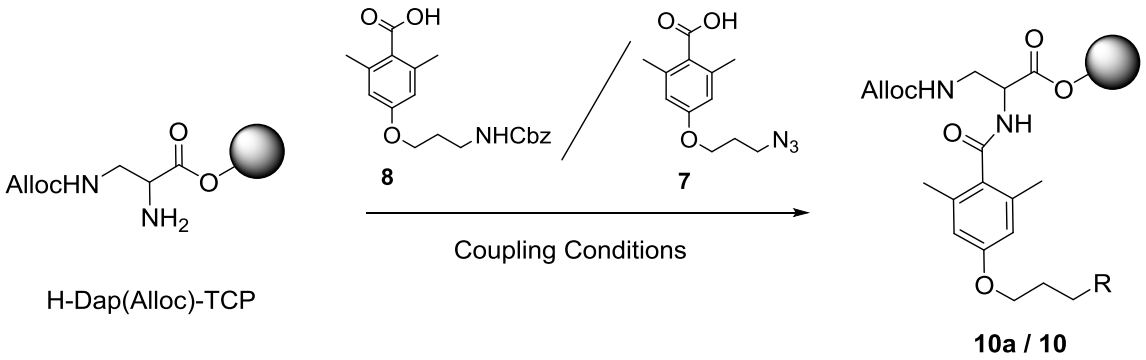

Compound	R-	Aromatic Acid	Coupling Condition	Solvent	Result
10a	-NHCbz	**8**	HBTU/HOBt/DIEA	NMP	-
10a	-NHCbz	**8**	HATU/HOAt/DIEA	NMP	-
10a	-NHCbz	**8**	TBTU/HOBt/DIEA	NMP	-
10a	-NHCbz	**8**	PyBrOP/DIEA	DCM	-
10	$-N_3$	**7**	HATU/HOAt/DIEA	NMP	-
10	$-N_3$	**7**	HATU/HOAt/DIEA	DMF	-
10	$-N_3$	**7**	HBTU/HOBt/DIEA	DMF	-
10	$-N_3$	**7**	PyBrOP/DIEA	DCM	-
10	$-N_3$	**7**	TCA, TPP, TEA	THF	>60%

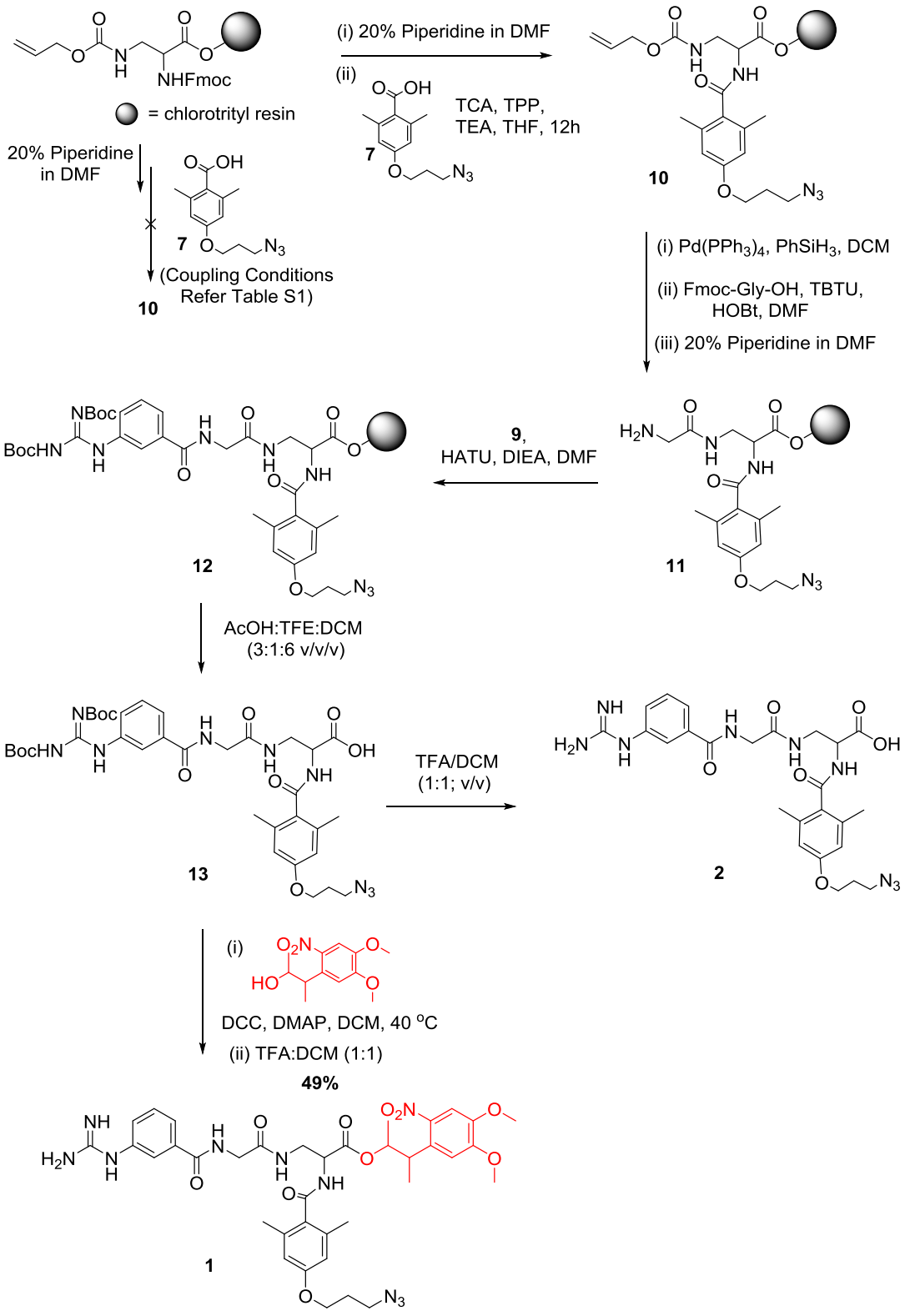

Scheme S2: Detailed scheme of synthesis of $\alpha_5\beta_1$ specific ligand (2) and its phototriggerable derivative (1).

(Z)-3-(2,3-bis(tert-butoxycarbonyl)guanidino)benzoic acid (9): To a solution of 3-aminobenzoic acid (500 mg, 3.64 mmol, 1 equiv.) in dry acetonitrile (10 mL), N,N'-bis-Boc-guanidinylpyrazole (3.4 g, 10.93 mmol, 3 equiv.) was directly added under inert conditions. The reaction mixture is then heated at 80 ^{o}C for 12 h. After the completion of the reaction, silica gel was added to the mixture and was purified using column chromatography (20% ethyl acetate in hexane) to afford the product as white solid (0.33 g, yield 80%). N,N'-bis-Boc-guanidinylpyrazole was recovered at 10% ethyl acetate in hexane, which could be recycled by concentration of the filtrate and recrystallization from hexane and ethyl acetate. TLC R_F (Hexane/EtOAc: 70/30) = 0.5. ^{1}H-NMR (300MHz, $CDCl_3$): δ/ppm = 10.40 (bs, acid), 8.21 (1H, s), 8.20-8.06 (1H, t, J= 8 Hz); 7.85-7.81 (1H, d, J= 8 Hz); 7.54-7.49 (1H, t, J= 8 Hz); 1.52 (s, 18H). ^{13}C-NMR (75 MHz, $CDCl_3$): δ/ppm = 168.05, 133.05, 130.69, 128.52, 127.50, 125.01, 29.14. ESI-MS/QTOF: 380.1818 ($M+H^+$).

Solid phase peptide synthesis (SPPS) Conditions

Solid phase peptide synthesis (SPPS) was carried out in syringe containing a frit disc that fits the syringe. The resin that binds the peptide is weighed and taken into the syringe. The reagents are drawn into the syringe and are shaken on a IKA KS 260 basic shaker at 300 rpm speed. After the completion of the reaction solution is pushed and drained out completely, later the resin bound molecule can be stored in the freezer with nozzle of the syringe closed.

3-(((allyloxy)carbonyl)amino)-2-(4-(3-azidopropoxy)-2,6-dimethylbenzamido)propanoic acid (Fmoc-Dap(Alloc)-OH) loading on TCP resin: After swelling the resin 100 mg of 2-Chlorotrityl chloride resin (100-200 mesh), 1% DVB resin (loading 0.151 mmol/100 mg) in dry DCM for 15 minutes, a solution of N-α-Fmoc-N-β-Alloc-l-diaminopropionic acid (0.074 mg) and N,N-diisopropylethylamine (DIEA, 65 µL, 2.5 equi.) in anhydrous DCM (2 mL) was taken into the syringe. Reaction was allowed to proceed at room temperature for 1 h. The remaining trityl chloride groups were capped by addition of a solution of MeOH/DIEA (4/1, v/v, 1 ml/g resin) for 15 min. The resin was filtered and washed thoroughly with DCM (2x), DMF (3x) and MeOH (5x). The loading capacity was determined by weight after drying the resin under vacuum. Loading of N-α-Fmoc-N-β-Alloc-l-diaminopropionic acid was calculated to be 0.83 mmol/g.

The loaded resin was subjected to Fmoc deprotection using condition described in **GP1**.

Coupling of (8) to H-Dap(Alloc)-TCP and Synthesis of (10):

The H-Dap(Alloc)- loaded resin (0.83 mmol/g) was taken into an round bottom flask, N_2 was flushed through the rubber septum for 2 minutes. After attaining inert atmosphere, dry THF (5 mL) was added into the flask. In another flask, aromatic acid **8** (48 mg, 0.166 mmol, 2 equiv.) was taken and 5 mL THF was added. The solution was cooled to 0 ^{o}C in ice. Triethylamine (56.6

µL, 0.415 mmol, 5 equiv.) followed by (24 µL, 0.25 mmol, 3 equiv.) and triphenylphosphine (65.2 mg, 0.25 mmol, 3 equiv.) was added to the solution. The mixture containing coupling agents were drawn from the flask using syringe and were added into the flask containing resin. The reaction was shaken for 12 h on the shaker with speed of 300 rpm. The conversion was followed by cleaving a small portion of the resin using **GP4** [ESI-MS/LC/MSD data provided below, Unreacted H-Dap(Alloc)-TCP = 189.0 ($M+H^+$), Coupled product 420.2 ($M+H^+$)]. After 12 h, the resin is then transferred back into a syringe containing fritted filter. The resin is washed with DCM (5 x 10 mL) followed by DMF (5 x 10 mL). The brown colour due to reaction lightens on repeated washing steps.

Unreacted amine groups were treated with acetic anhydride (30 equiv.) and trimethylamine (50 equiv.) in DMF for 30 minutes. Resin was then washed with DMF (5 x 5 mL), followed by DCM DMF (3 x 5 mL) before proceeding for Alloc deprotection.

Synthesis of (10-13): Alloc deprotection is carried out using reported procedure using tetrakis-triphenylphosphinepalladium and phenylsilane in DCM.[1] The amine obtained on the resin is then coupled with Fmoc-Gly-OH using TBTU as described in **GP2**, followed by Fmoc deprotection as in **GP1** and the obtained amine **11** was then coupled with compound **9** using HATU as in **GP2**. Cleavage of the peptide to obtain Diboc protected derivative **13** from TCP resin was achieved by **GP3**.

2-(4-(3-azidopropoxy)-2,6-dimethylbenzamido)-3-(2-(3-guanidinobenzamido)acetamido) propanoic acid (2): To obtain compound **2**, compound **13** is subjected to Boc deprotection using **GP4**. ESI-MS/QTOF: 554.2468 ($M+H^+$).

3-(4,5-dimethoxy-2-nitrophenyl)butan-2-yl 2-(4-(3-azidopropoxy)-2,6-dimethylbenzamido)-3-(2-(3-guanidinobenzamido)acetamido)propanoate (1): To a solution of **13** (1.5 mg, 1.99 mmol, 1 equiv.) in dry DCM (1 mL) was subsequently added at 0 °C 3-(4,5-dimethoxy-2-nitrophenyl)butan-2-ol (DMNPB, 0.76 mg, 2.98 mmol, 1.5 equiv.), DCC (1.02 mg, 4.98 mmol, 2.5 equiv.), and DMAP (0.6 mg, 4.98 mmol, 2.5 equiv.). After 30 minutes, reaction was warmed at 40 °C for 12 h, with a reflux condenser attached. Reaction progress was monitored in analytic HPLC using a gradient of 30B-95B in 40 minutes (0-3 min - 30% B; 3-22 min – 30% - 95% B; hold 3 min 95%B). TFA in DCM (1:1 v/v) is added and stirred for about 30 minutes. DCM was evaporated under N_2 stream and semipreparative HPLC purification yielded compound **1** (1.05 mg, 49%). ESI-MS/QTOF: 791.3458 ($M+H^+$).

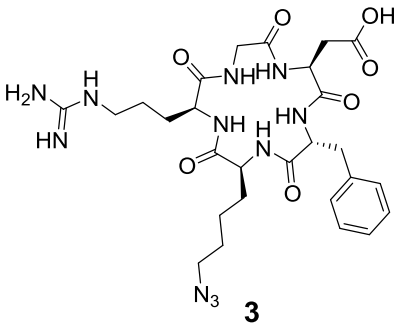

3

cy[RGDfK(N_3)]

Scheme S3: Structure of cy[RGDfK(N_3)] **3**.

3-(4,5-dimethoxy-2-nitrophenyl)butan-2-yl 2-((2S,5R,8S,11S)-8-(4-azidobutyl)-5-benzyl-11-(3-guanidinopropyl)-3,6,9,12,15-pentaoxo-1,4,7,10,13-pentaazacyclopentadecan-2-yl)acetate (3, cy[RGDfK(N_3)]): Compound **3** was obtained from GeneCust Europe by custom peptide synthesis. ESI-MS/LC/MSD: 629.8 ($M+H^+$), 651.8 ($M+H^+$).

Photochemical studies

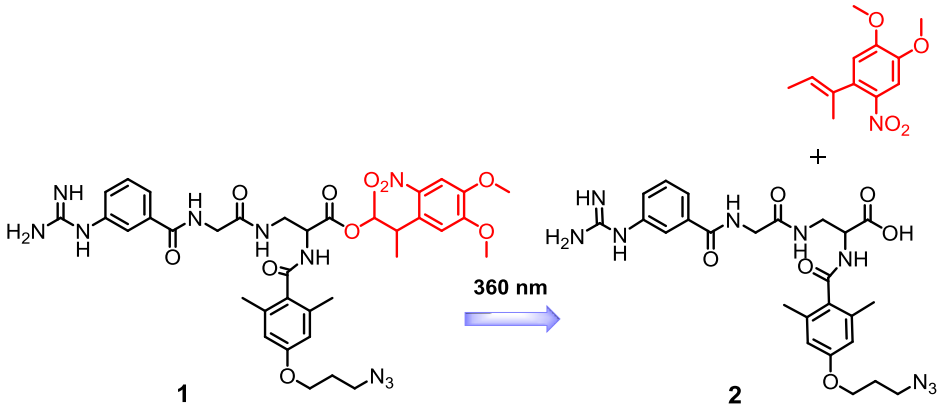

Scheme

A 0.5 mM solution of compound **1** in water (0.5 ml) was irradiated at 360 nm (2.7 mW/cm^2) with LUMOS 43 LED (Atlas Photonics Inc).

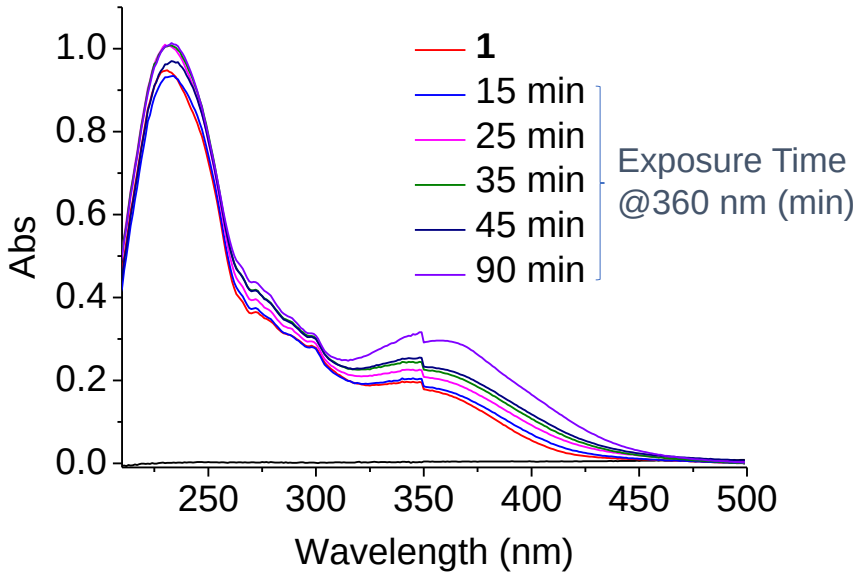

Figure S1: UV spectra of **1** after irradiation at 360 nm with increasing times at 360 nm (2.7 mW/cm^2).

The quantitative analysis of irradiated samples was carried out by reverse phase HPLC. After diluting the aliquot with 80 µL solution solvent B used in HPLC (95% ACN, 5% H_2O and 0.1% TFA). The solvent gradient used to record chromatogram was 0-3 min - 5% B; 3-22 min – 5% - 95% B; hold 3 min 95%B. The solvent A comprised H_2O and 0.1% TFA.

Surface Functionalization Strategy for different ligands:

NEXTERION® H glass slide (Schott, Geramny) functionalized with reactive -NHS group was incubated for 3 h with 1 mM solution of Dibenzocyclooctyne-amine (DBCO) in DMSO. Substrate was washed with water three times and dried carefully by rolling the water droplets away and gently tapping to get rid of the tiny droplets. A 12-well Ibidi® silicon gasket was mounted on Nextrion slide to compartmentalize the surface in order to test different conditions on same e slide. Ddifferent concentration (0.005 – 0.05 $mgmL^{-1}$) of azide termined ligands solutions (in water) were added (40 µL) and allowed to react for 3h at r.t or overnight at 4 °C.

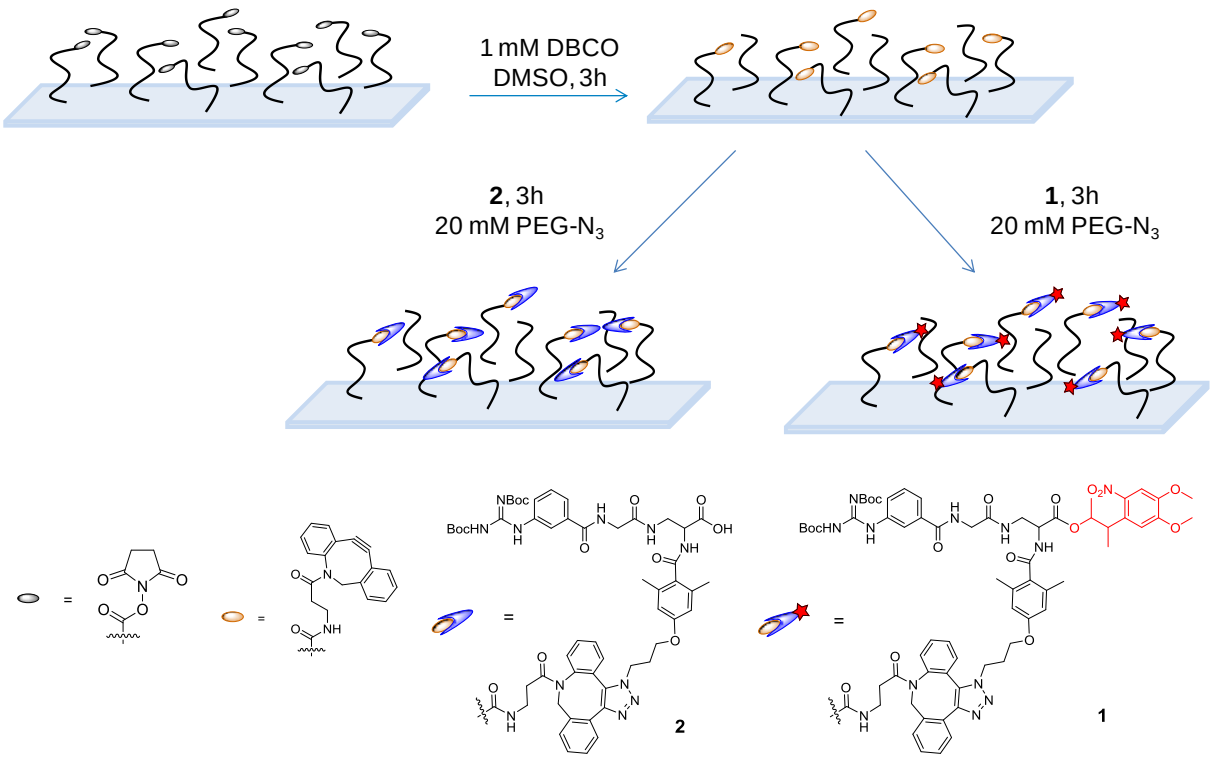

Scheme 4: Steps involved in covalently immobilizing azide terminating ligands to the NEXTERION® H glass slide.

Photoactivation of Functionalized Surface for Cell Assays

Photoactivation of photoactivatable-$\alpha_5\beta_1$-ligand **1** modified substrate was carried out by using a Polychrome coupled to a Xe-lamp (TILL Photonics GmbH, Gräfelfing, Germany) by irradiation at 360 nm (0.3 $mWcm^{-2}$). Samples were either fully uncaged or irradiated through a quartz mask with stripes of 300 µm glass with 600 µm chrome (ML&C, Jena, Germany) for 6 min. After irradiation substrates were washed with water in order to remove the side products from the photocleavage from the surface. Substrates were sterilized by washing with ethanol and washed 3 times with PBS before cell seeding.

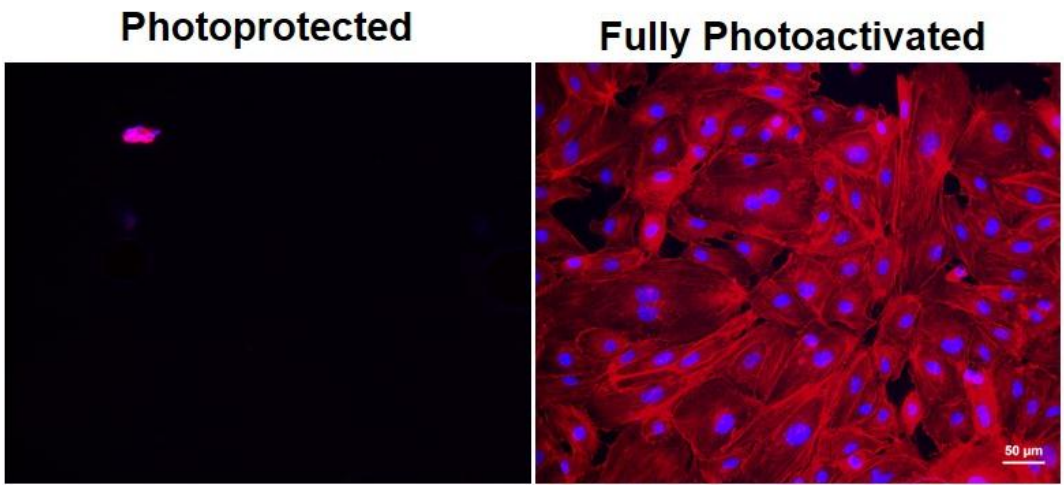

Figure S2: Immunofluorescence images of HUVECs cultured Nexterion® H glass slide functionalized with photoactivatable-$\alpha_5\beta_1$-ligand **1** and on fully activated substrate.

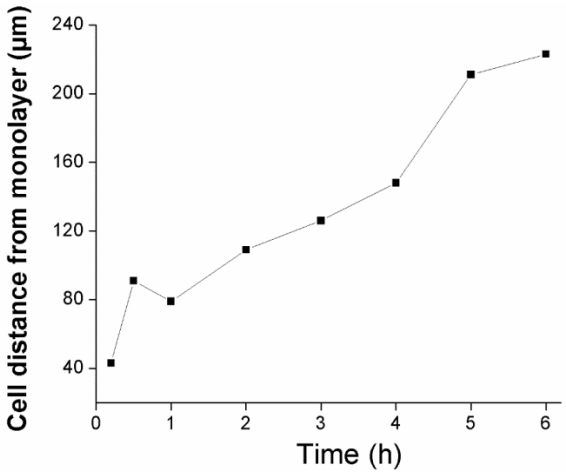

Figure S3: Migration path (40x 250 µm) was *in-situ* activated in front of the monolayers by using 405 nm scanning laser from a microscope.

NMR Data:

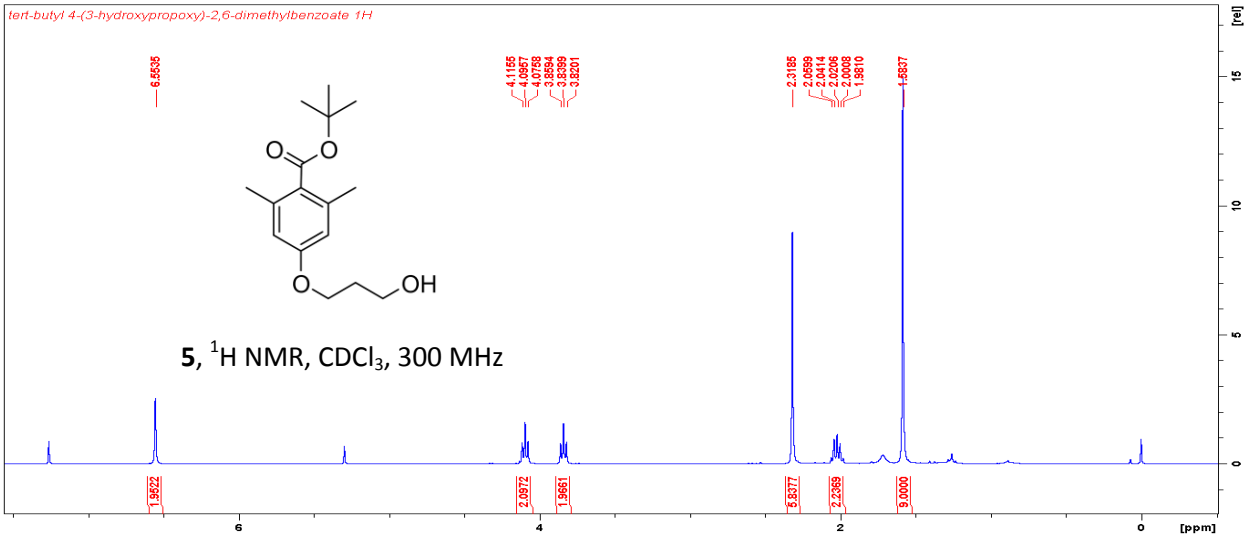
tert-butyl 4-(3-hydroxypropoxy)-2,6-dimethylbenzoate 1H
6.5535
4.1155
4.0967
4.0758
3.8594
3.8399
3.8201
2.3185
2.0599
2.0414
2.0206
2.0008
1.9810
1.6837
1.9522
2.0972
1.9661
5.8377
2.2369
9.0000
OH
5, 1H NMR, CDCl3, 300 MHz
[ppm]
[rel]

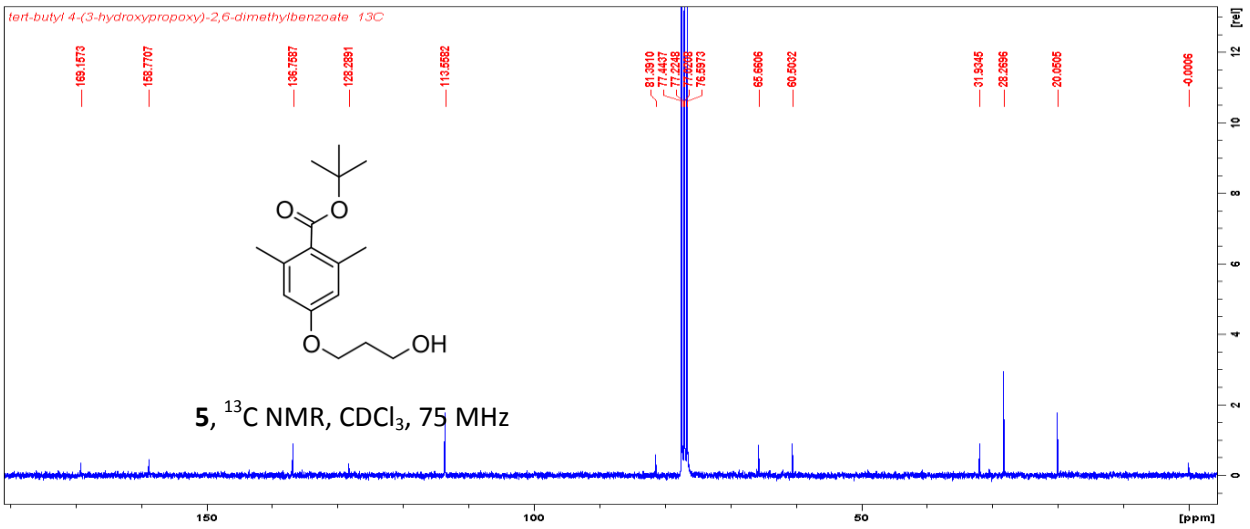
tert-butyl 4-(3-hydroxypropoxy)-2,6-dimethylbenzoate 13C
168.1573
158.7707
136.7587
128.2891
113.5582
81.3910
77.4437
77.2248
76.5870
65.6606
60.5032
31.9345
28.2696
20.0505
-0.0006
OH
5, 13C NMR, CDCl3, 75 MHz
[ppm]
[rel]

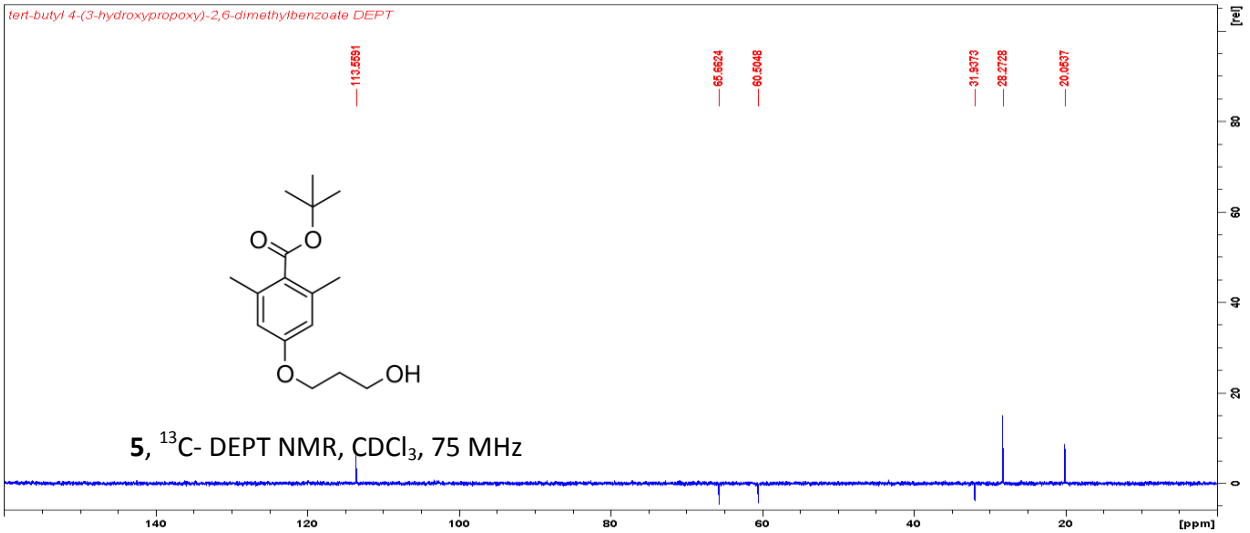
tert-butyl 4-(3-hydroxypropoxy)-2,6-dimethylbenzoate DEPT
113.5591
65.6624
60.5048
31.9373
28.2728
20.0537
OH
5, 13C- DEPT NMR, CDCl3, 75 MHz
[ppm]
[rel]

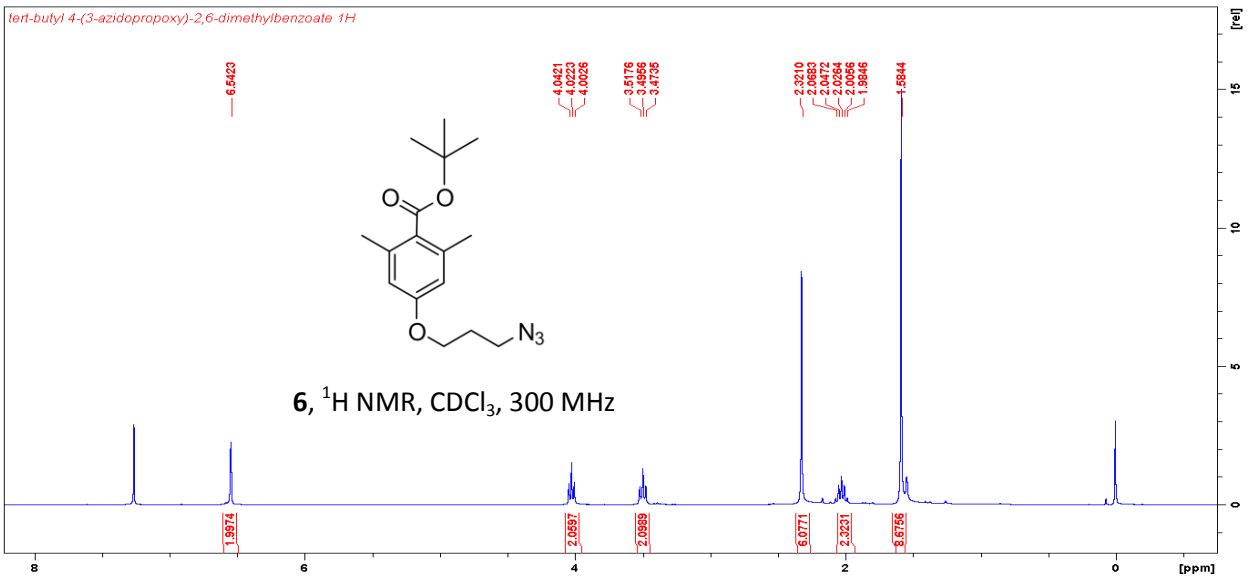

6, ^{1}H NMR, $CDCl_3$, 300 MHz

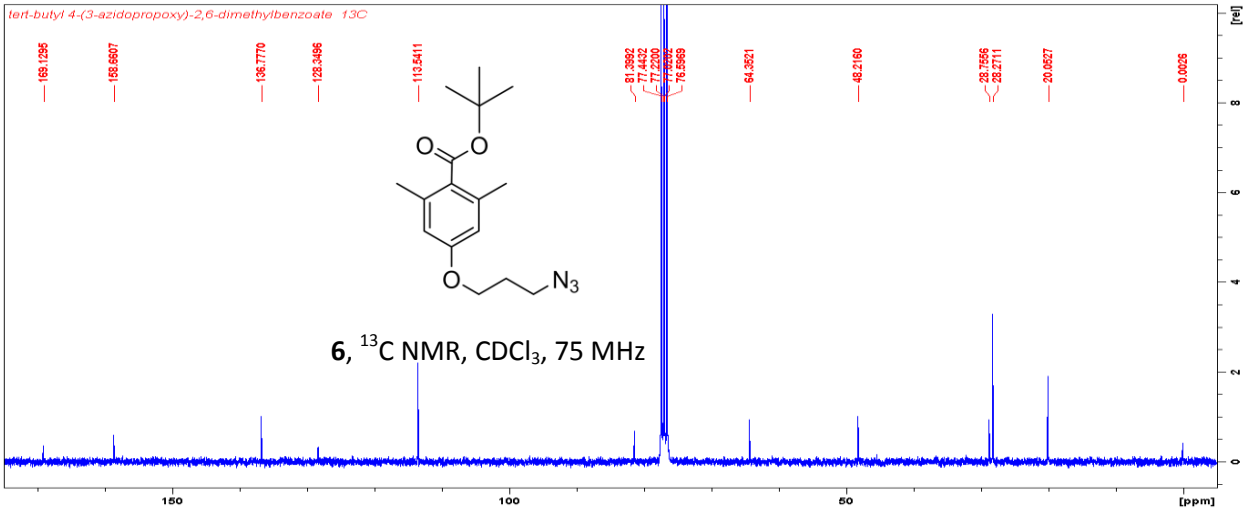

6, ^{13}C NMR, $CDCl_3$, 75 MHz

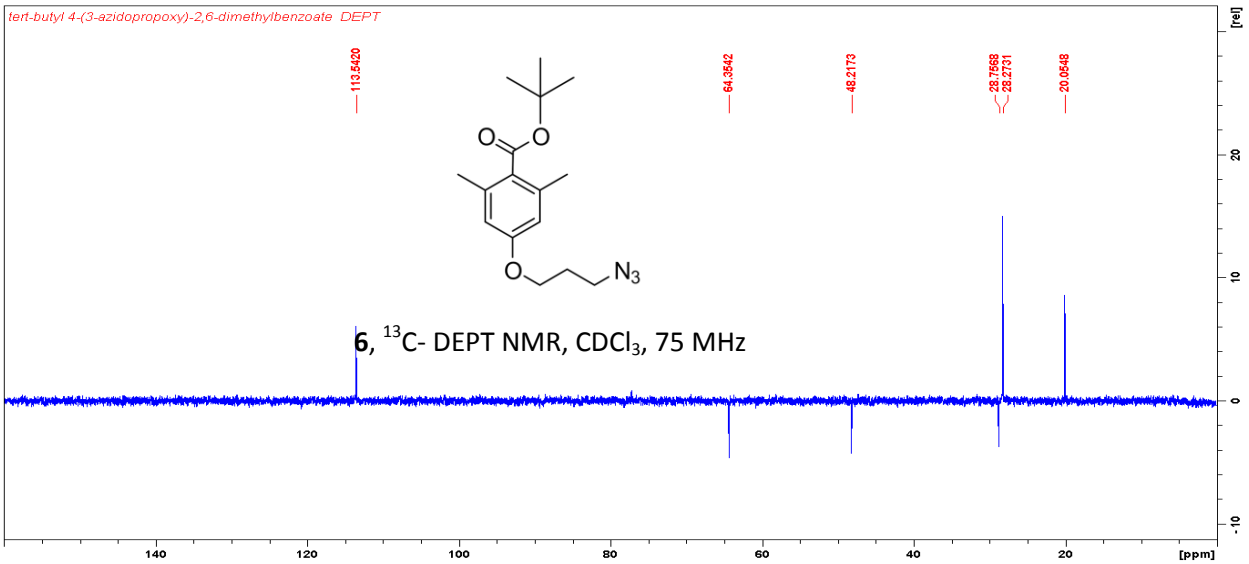

6, ^{13}C- DEPT NMR, $CDCl_3$, 75 MHz

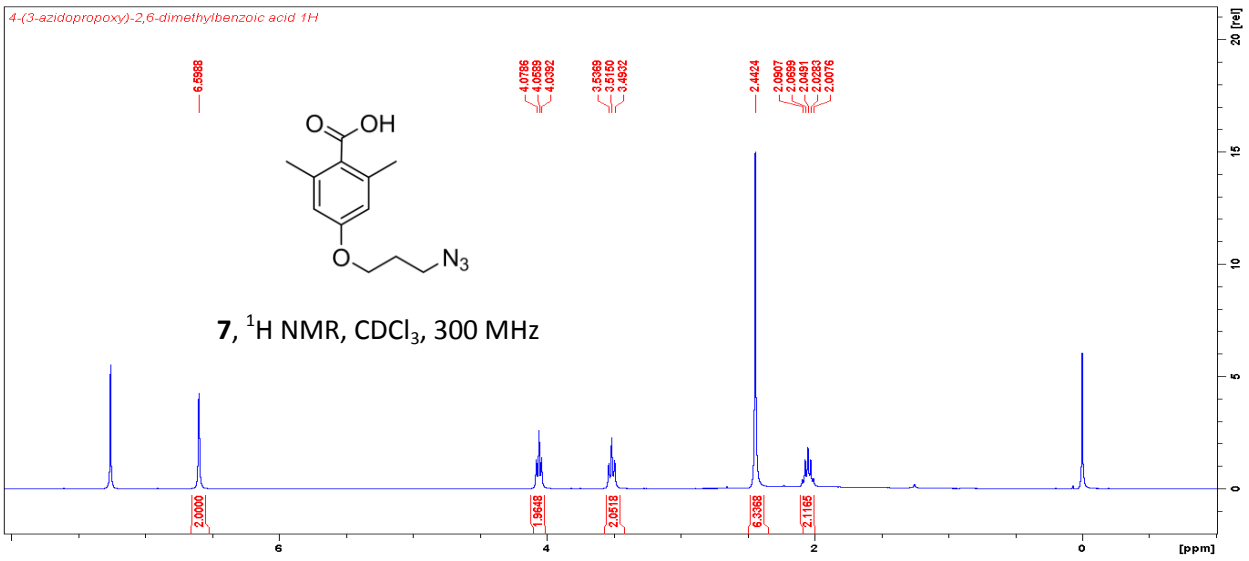

7, ^{1}H NMR, $CDCl_3$, 300 MHz

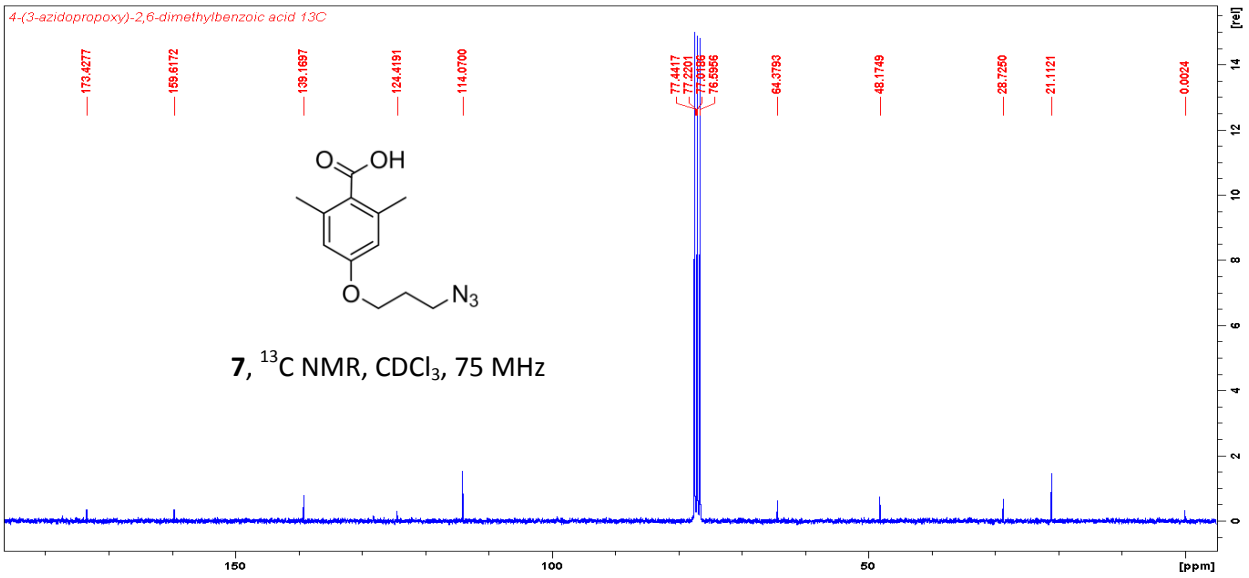

7, ^{13}C NMR, $CDCl_3$, 75 MHz

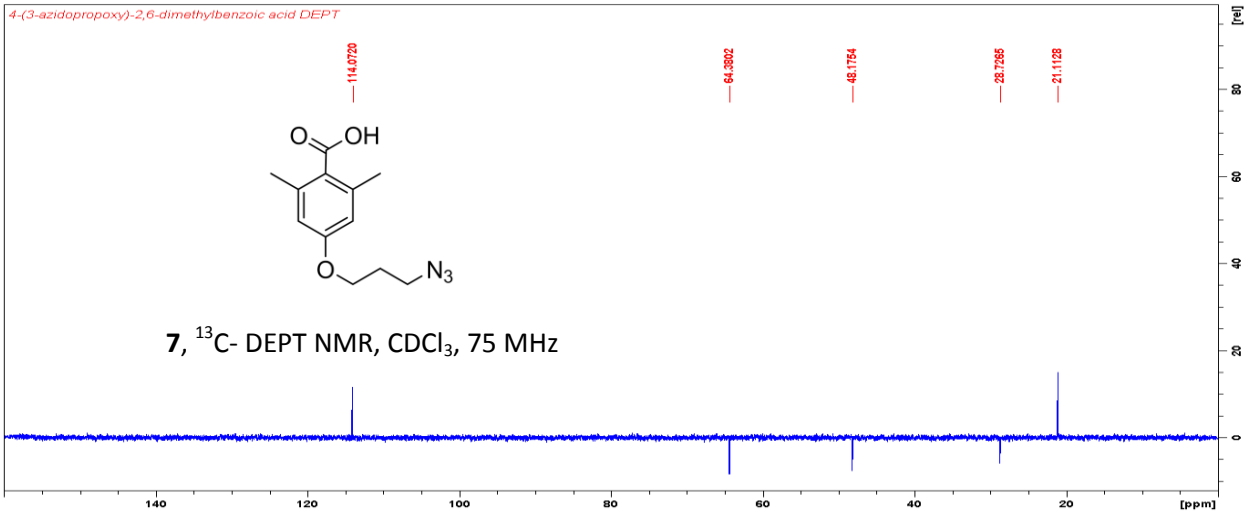

7, ^{13}C- DEPT NMR, $CDCl_3$, 75 MHz

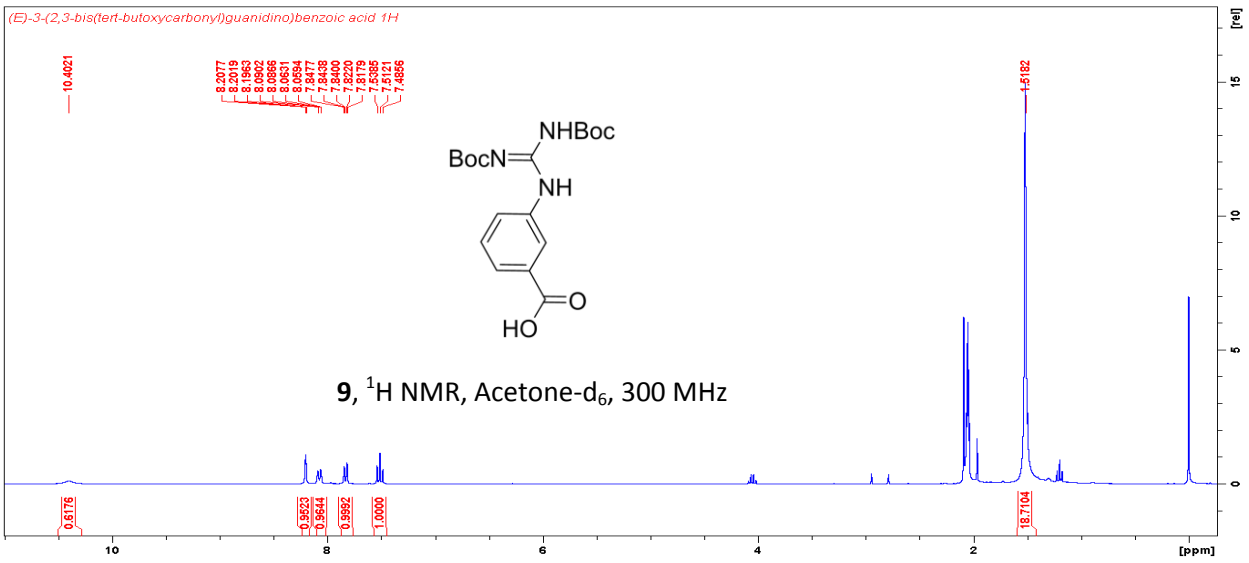

9, ^{1}H NMR, Acetone-d$_6$, 300 MHz

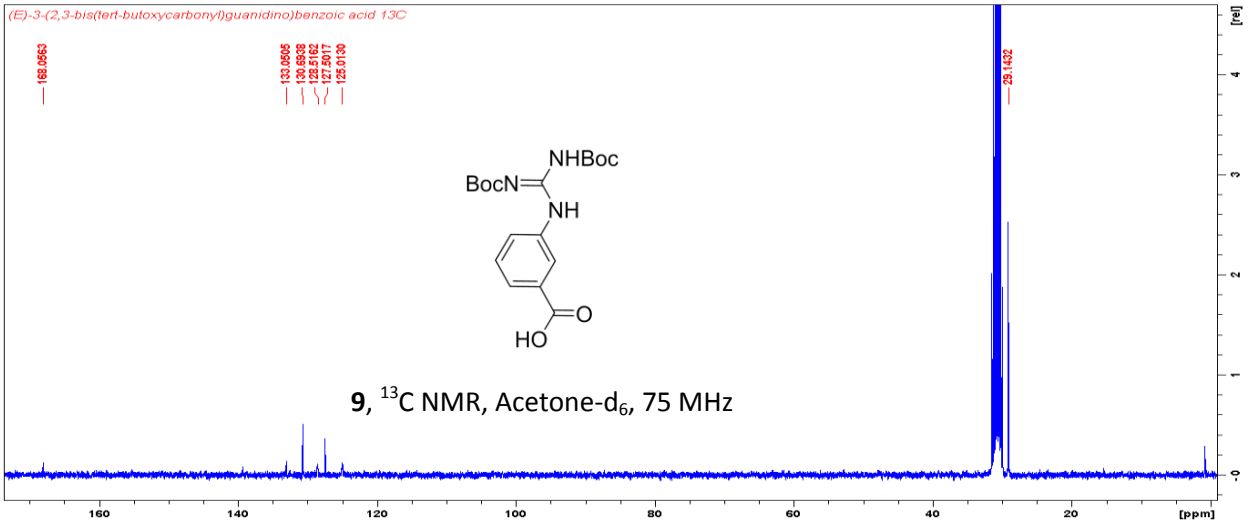

9, ^{13}C NMR, Acetone-d$_6$, 75 MHz

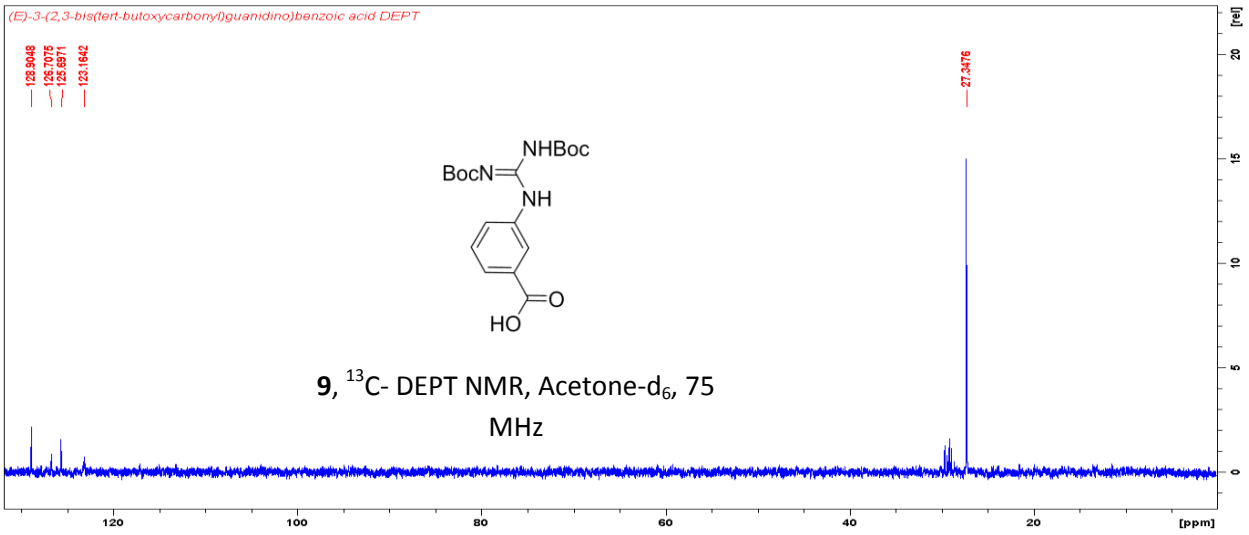

9, ^{13}C- DEPT NMR, Acetone-d$_6$, 75 MHz

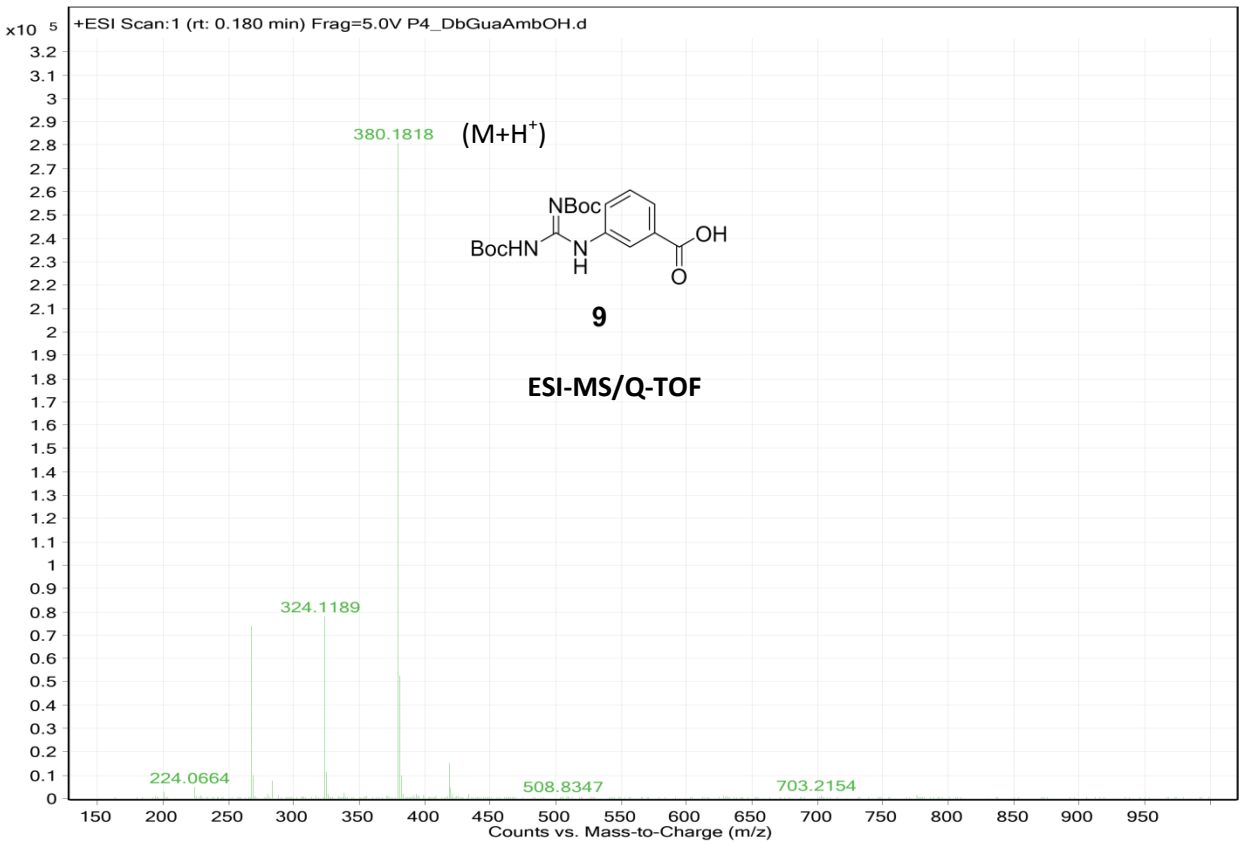
+ESI Scan:1 (rt: 0.180 min) Frag=5.0V P4_DbGuaAmbOH.d
x10 5
380.1818
(M+H+)
NBoc
BocHN
N
H
OH
O
9
ESI-MS/Q-TOF
324.1189
224.0664
508.8347
703.2154
Counts vs. Mass-to-Charge (m/z)

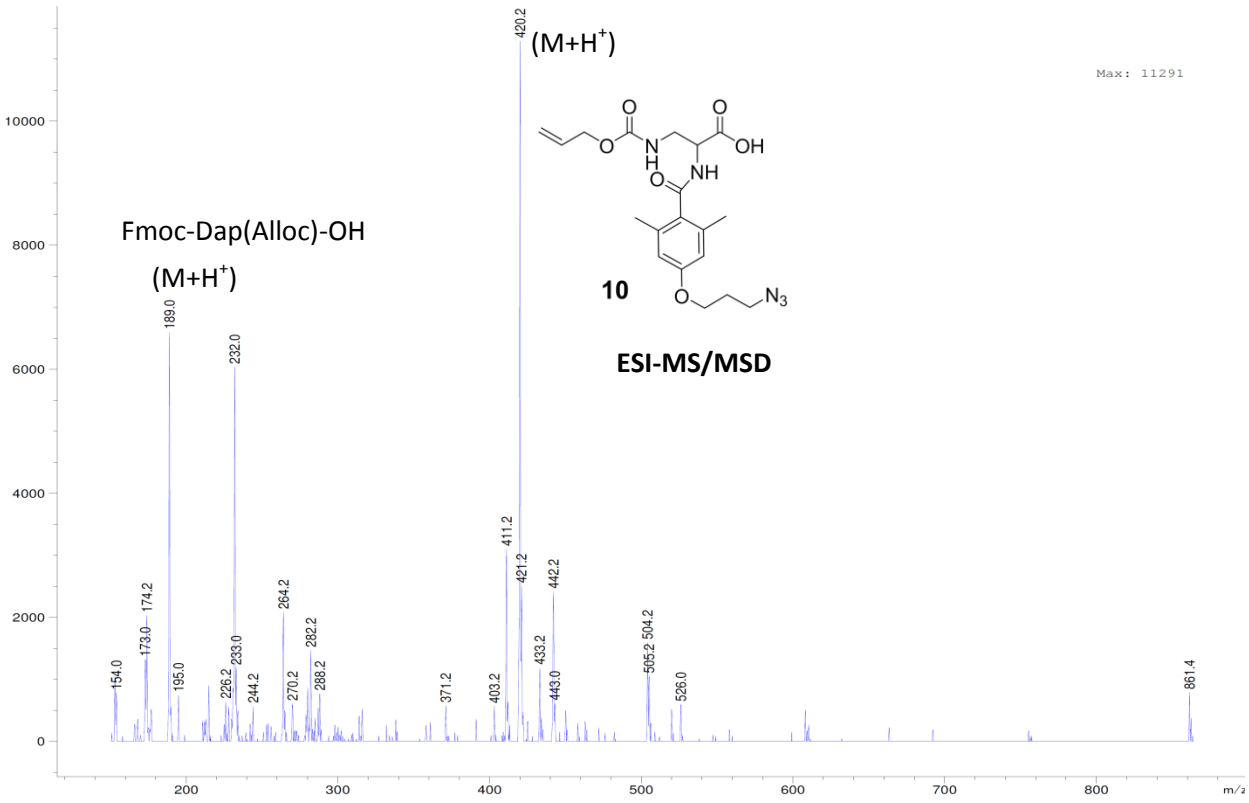
Fmoc-Dap(Alloc)-OH
(M+H+)
420.2
(M+H+)
Max: 11291
10
ESI-MS/MSD
189.0
232.0
174.2
173.0
154.0
195.0
226.2
233.0
244.2
264.2
270.2
282.2
288.2
371.2
403.2
411.2
421.2
433.2
442.2
443.0
505.2
504.2
526.0
861.4
m/z

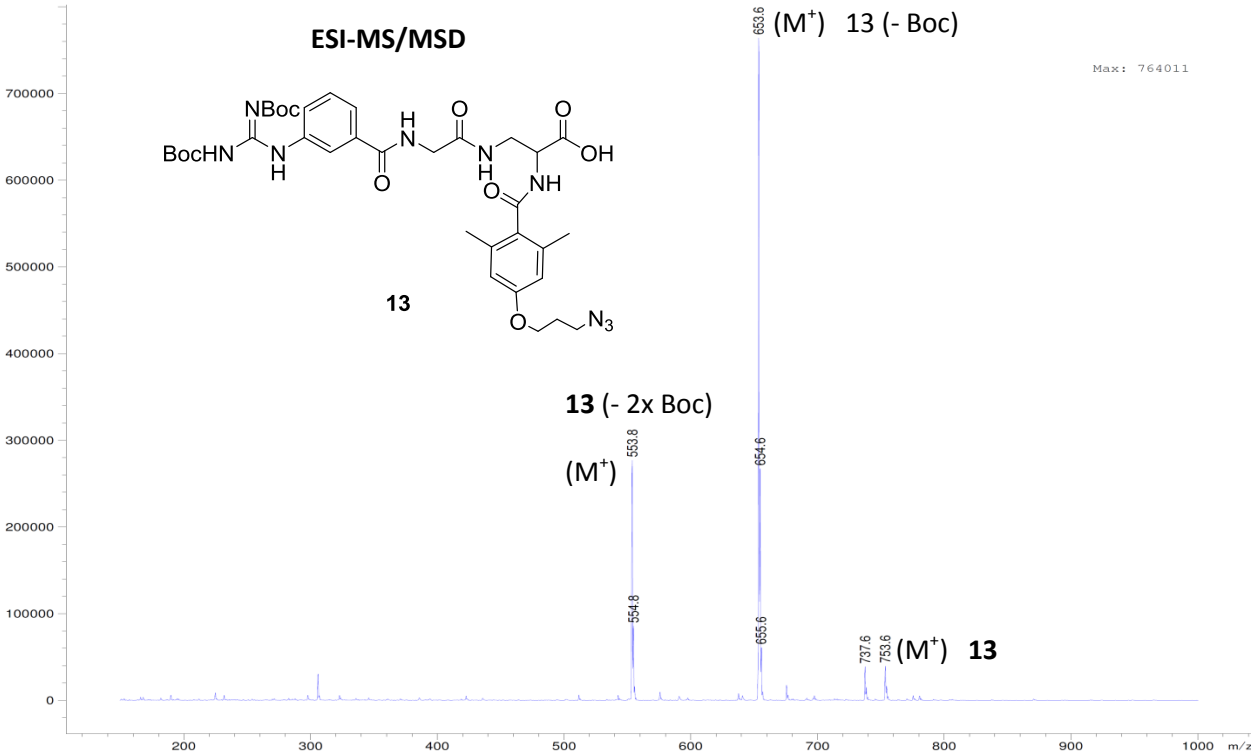
ESI-MS/MSD
653.6 (M+) 13 (- Boc)
Max: 764011
NBoc
BocHN
OH
NH
13
13 (- 2x Boc)
(M+)
553.8
654.6
554.8
655.6
737.6
753.6
(M+) 13
700000
600000
500000
400000
300000
200000
100000
0
200
300
400
500
600
700
800
900
1000
m/z

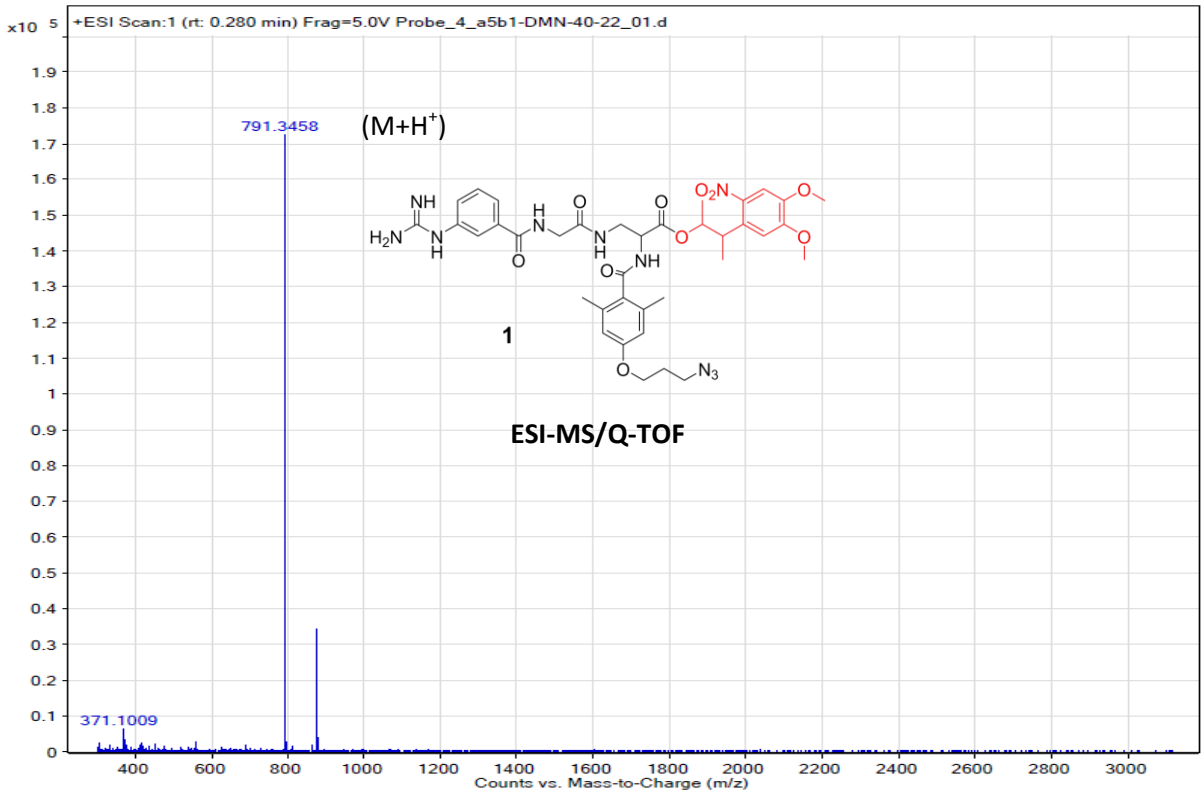
x10 5
+ESI Scan:1 (rt: 0.280 min) Frag=5.0V Probe_4_a5b1-DMN-40-22_01.d
791.3458
(M+H+)
1
ESI-MS/Q-TOF
371.1009
Counts vs. Mass-to-Charge (m/z)

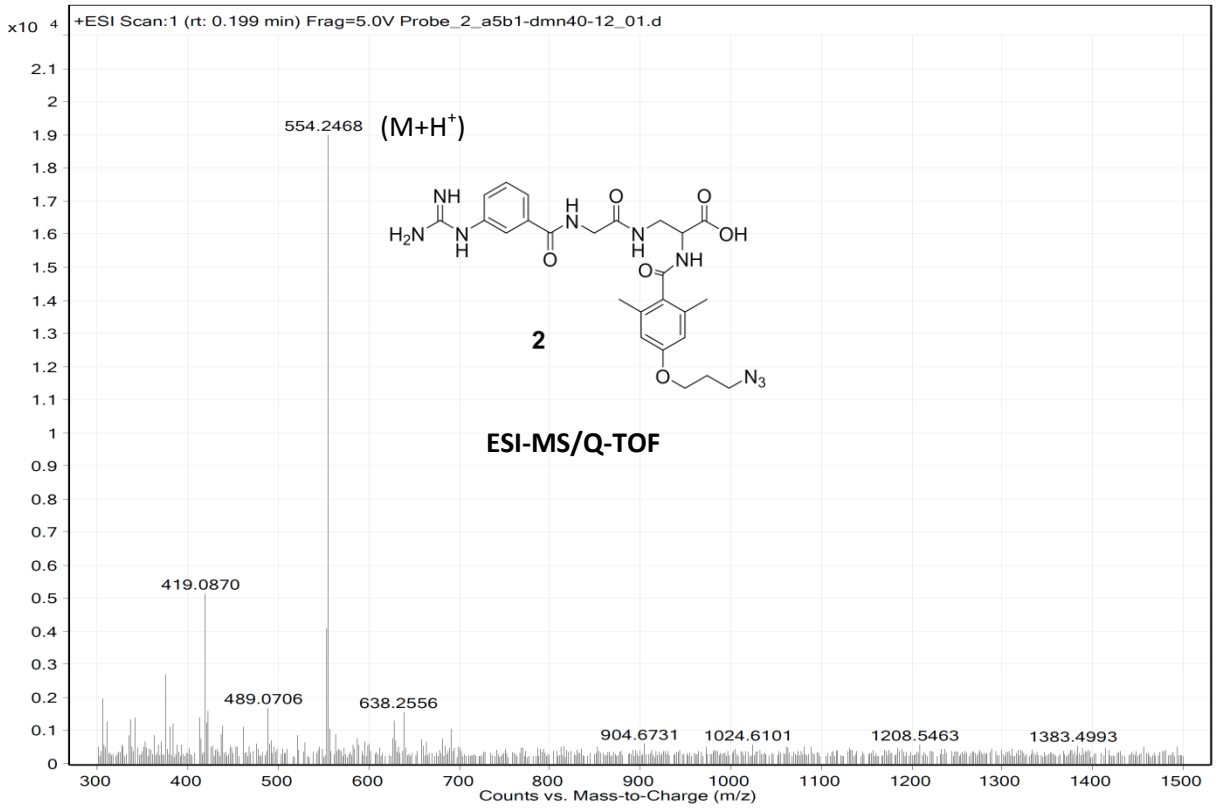
+ESI Scan:1 (rt: 0.199 min) Frag=5.0V Probe_2_a5b1-dmn40-12_01.d
x10 4
554.2468
(M+H+)
2
ESI-MS/Q-TOF
419.0870
489.0706
638.2556
904.6731
1024.6101
1208.5463
1383.4993
Counts vs. Mass-to-Charge (m/z)

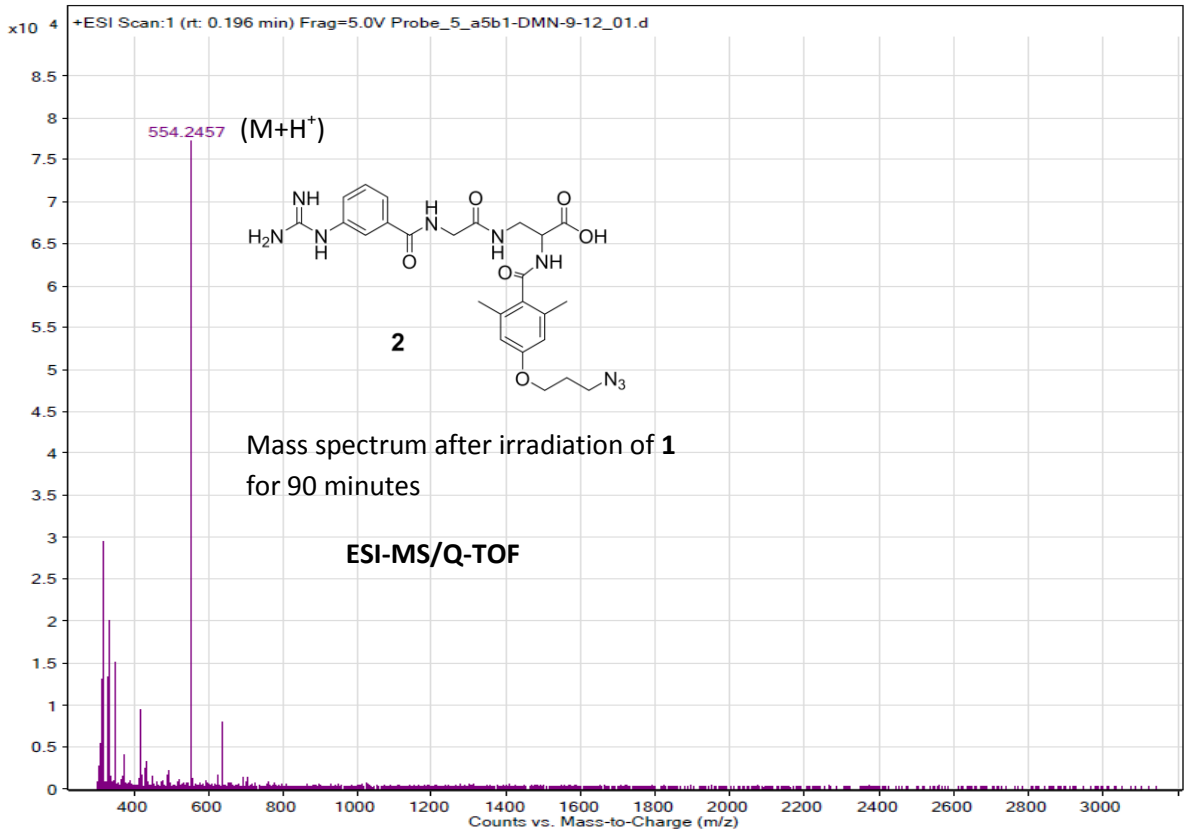
+ESI Scan:1 (rt: 0.196 min) Frag=5.0V Probe_5_a5b1-DMN-9-12_01.d
x10 4
554.2457
(M+H+)
2
Mass spectrum after irradiation of 1
for 90 minutes
ESI-MS/Q-TOF
Counts vs. Mass-to-Charge (m/z)

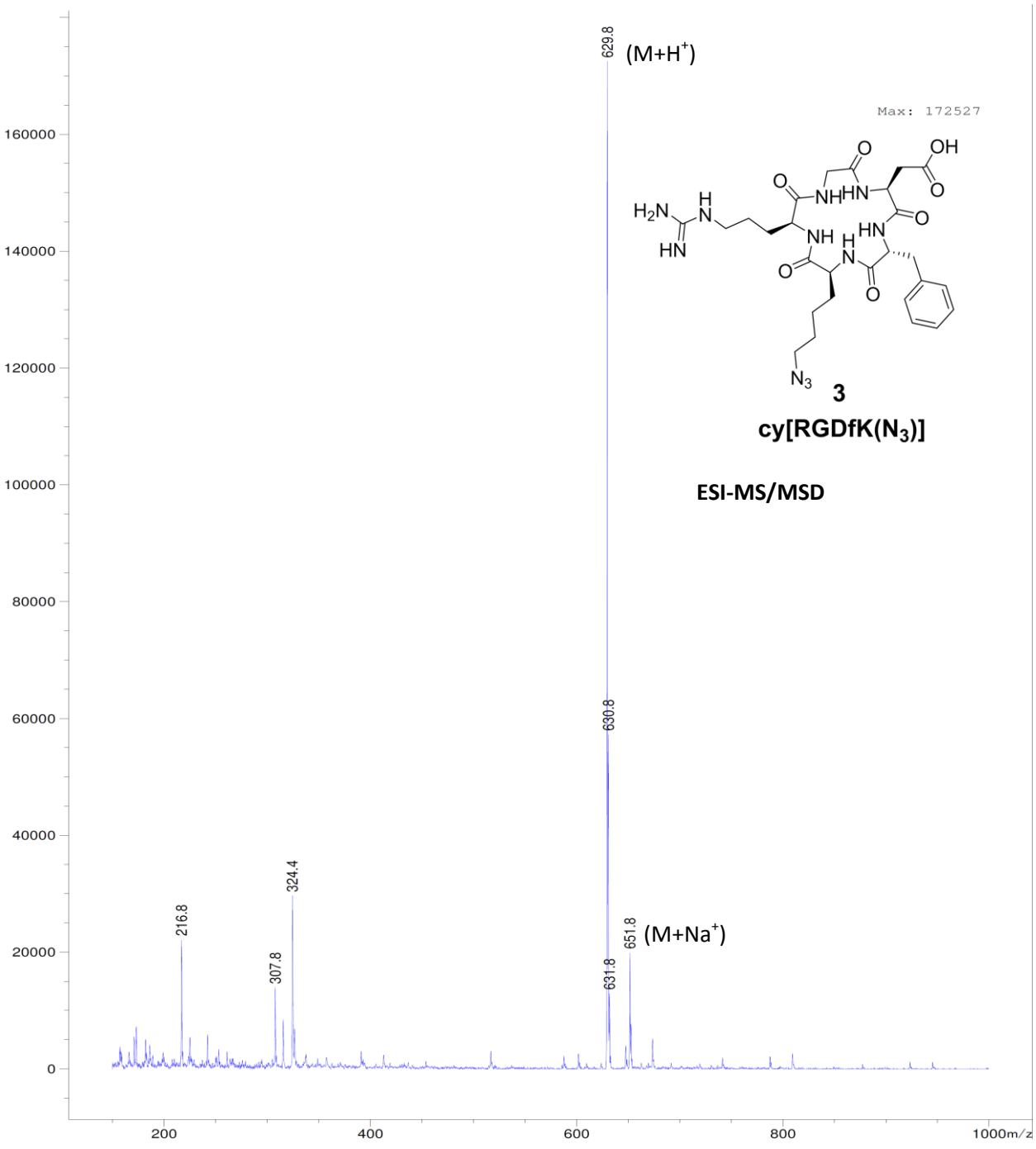

Reeferences:

[1] F. Rechenmacher, S. Neubauer, J. Polleux, C. Mas-Moruno, M. De Simone, E. A. Cavalcanti-Adam, J. P. Spatz, R. Fassler, H. Kessler, *Angew. Chem. Int. Ed.* **2013**, *52*, 1572-1575.

[2] A. S. Thompson, G. R. Humphrey, A. M. DeMarco, D. J. Mathre, E. J. J. Grabowski, *J. Org. Chem.* **1993**, *58*, 5886-5888.